

Path Tracking of a UAV via an Underactuated \mathcal{H}_∞ Control Strategy

Guilherme V. Raffo*, Manuel G. Ortega**, Francisco R. Rubio***

Department of Systems Engineering and Automation, University of Seville, Camino de los Descubrimientos sn, 41092 Seville, Spain

In this study, a nonlinear robust control strategy designed for underactuated mechanical systems is proposed in order to solve the path tracking problem for a quadrotor unmanned aerial vehicle. An underactuated nonlinear \mathcal{H}_∞ controller based on the six degrees of freedom dynamic model is designed to control the helicopter attitude and altitude in the inner-loop. The outer-loop control is performed using a model-based predictive controller (MPC) to track the reference trajectory. The robust performance achieved with the proposed control strategy is checked by simulation in the presence of aerodynamic disturbances, unmodelled dynamics and parametric uncertainties.

Keywords: Nonlinear \mathcal{H}_∞ control, predictive control, robust control, underactuated mechanical system, autonomous aerial vehicle

1. Introduction

The quadrotor unmanned aerial vehicle (UAV) is an autonomous four rotor helicopter, which is often used to develop control laws for VTOL (Vertical Take-Off and Landing). Besides, the quadrotor UAV configuration presents some advantageous features in comparison with the standard helicopter one. This is mainly because it is lifted and propelled by four rotors, which makes it possible to reduce each individual rotor size and to maintain or to increase the total UAV load capacity, when compared

with a helicopter with one main rotor. Furthermore, these vehicles do not require complex mechanical linkages to act on propellers. This reduces the design, maintenance and cost of the vehicle [15]. These facts, added to its high maneuverability, allow take-offs and landings, as well as flight in tough environment.

The quadrotor helicopter tries to reach a stable hovering and flight using the equilibrium forces produced by the four rotors [7]. The movement of the UAV results from changes in the angular speed of the rotors. Longitudinal motions are achieved by means of changes in the front and rear rotor velocity, while lateral displacements are performed using the speed of the right and left propellers. Yaw movement is obtained from the difference in the counter-torque between each pair of propellers, i.e., accelerating the two clockwise turning rotors while decelerating the counter-clockwise turning rotors, and vice-versa.

Nevertheless, these kind of vehicles are underactuated mechanical systems with six degrees of freedom (DOF) and only four control actions, which complicates the control design stage. Techniques developed for fully actuated robots can not be directly applied to underactuated nonlinear mechanical systems [10]. Therefore, nonlinear modelling techniques and modern nonlinear control theory are usually employed to achieve autonomous flight with high performance [16], [7], [12].

Several studies have been published describing some control strategies to solve the path tracking problem for the quadrotor helicopter. In [21], the path tracking problem was solved using exact linearization techniques via dynamic feedback. In [9], the angular rates and vertical velocity stabilization by a 2DOF \mathcal{H}_∞ controller using

*Correspondence to: G.V. Raffo, E-mail: raffo@cartuja.us.es

**E-mail: ortega@cartuja.us.es

***E-mail: rubio@cartuja.us.es

Received 28 September 2009; Accepted 2 June 2010

Recommended by G.R. Damm, A.J. van der Schaft

the loop shaping technique was applied in the inner-loop. The same technique was used to control the longitudinal and lateral velocities, the yaw angle and the height in the outer-loop. A predictive control was designed to solve the path tracking problem in that study. Backstepping and sliding mode techniques were used to control the helicopter in [2]. In these strategies the model was split up into the angular rotations subsystem and the linear translations one. Xu and Özgüner proposed an approach using sliding mode control for underactuated mechanical systems to stabilize a quadrotor helicopter ([38],[39]). Robust feedback linearization with a \mathcal{H}_∞ controller was applied to perform the path tracking problem in [22]. In [23] a feedback linearization-based controller with a sliding mode observer was designed for the quadrotor helicopter.

The same model structure presented in [2] was used to design the controllers in [27], [28]. In [27] a control law based on a standard backstepping approach for translational movements and a fully actuated nonlinear \mathcal{H}_∞ controller to stabilize the helicopter were combined to perform path following in the presence of aerodynamic moments disturbances and parametric uncertainties. In [28] the same nonlinear \mathcal{H}_∞ controller presented in [27] was used to stabilize the UAV, while a predictive controller was employed to control the translational motion and to provide a smooth path tracking through its predictive features. However, both these strategies are only able to reject sustained disturbances applied to the rotational motion.

Although, several control strategies have been tested on the quadrotor helicopter, most of them do not consider external disturbances on the six degrees of freedom, unmodelled dynamics and parametric uncertainty on the whole model. For example, in [2], [6], [40] the proposed controllers are not capable to reject sustained disturbances. In [21] just disturbances on the translational movements were considered, and in [27], [28] disturbances are only taken into account in the rotational controller design.

In this study, the quadrotor helicopter path tracking is performed using a nonlinear \mathcal{H}_∞ control designed for underactuated mechanical systems in the inner-loop. This controller considers the overall dynamic behaviour in order to control the helicopter attitude and altitude. This fact implies that the translational and rotational motion control are not considered separately, being that their coupling are not treated like external disturbances. Therefore, this approach constitutes a clear advantage with respect to other control strategies proposed in the literature (e.g. [3], [27], [28]). Moreover, the underactuated nonlinear \mathcal{H}_∞ control proposed in this study makes it possible to reject persistent disturbances on the six degrees of freedom.

The proposed controller is based on the ones developed in [34] and in [25]. In [34] a nonlinear \mathcal{H}_∞ control for underactuated manipulators, by using the state tracking

error equation presented in [17], is proposed. Nevertheless, these results exhibit some main restrictions, as, for example, the assumption of null-average disturbances and an exact robot model. In [25] a nonlinear \mathcal{H}_∞ controller for fully actuated manipulator is developed, where the integral of the error position is added to the tracking error vector. In the same publication, conditions to formulate the controller in the form of a nonlinear PID were established, where the control signal can be penalized, as well as the error signals, their integral and their derivative. The nonlinear \mathcal{H}_∞ control considers a Hamilton-Jacobi-Bellman-Isaacs partial differential equation (HJBI PDE), which replaces the Riccati equation in the case of the linear \mathcal{H}_∞ control formulation. The main problem with the nonlinear case is that there is no general method to solve these HJBI PDEs. Therefore, solutions have to be found for each particular case. By applying game theory to formulate the nonlinear \mathcal{H}_∞ control, a constant gain similar to the results obtained with feedback linearization procedures is provided by an analytical solution. An explicit global parameterized solution to this problem, formulated as a minimax game, was developed in [8] for the particular case of mechanical systems formulated via Euler-Lagrange equations, which was modified in [34] and in [25].

In this study, both techniques are combined and adapted for the case of a quadrotor helicopter in order to synthesize the inner-loop controller. In the outer-loop an integral predictive controller is designed by determining the roll and pitch reference angles for the inner-loop controller. The outer-loop controller is an improvement of the one proposed in [28], since the integral action is added to the xy motion control law to deal with sustained disturbances. Furthermore, it provides a smooth path tracking due to the fact that the MPC formulation allows the use of previously known references for the control law calculation.

For the control strategy proposed in this study, it is assumed that all states are accessible by the controllers. Generally, it can result in difficulties for practical implementations. At the same time, there are a large variety of sensors available that provide the necessary measurements. For instance, Euler angles and angular velocities can be obtained through Inertial Measurement Systems. Besides, if it is combined with GPS (or differential GPS) the linear position and linear velocity can also be measured. At this stage it is necessary to keep in mind the objectives of the application such as, for example, if the UAV must fly in an indoor or outdoor environment, or if the GPS accuracy is admissible. Other kinds of sensors can be also used to estimate the UAV position and attitude, like ultrasound systems in a structured environment ([31]), vision systems ([1], [20], [35], [13]) and 3D tracker system (POLHEMUS) ([6], [14]).

The remainder of the study is organized as follows: in Section 2, a description of the quadrotor helicopter modelling is given. The control strategy used to perform the quadrotor helicopter path tracking is described in Section 3. The nonlinear \mathcal{H}_∞ controller formulated for underactuated mechanical system is developed in Section 4. In Section 5, a predictive controller for the outer-loop is presented. Some simulation results are shown in Section 6. Finally, the major conclusions of the work are drawn in Section 7.

2. System Modelling

2.1. Description

The dynamic model of the system is obtained under the hypothesis that the vehicle is a rigid body in the space subject to one main force (thrust) and three torques.

Due to the complexities presented, some assumptions are made for control purposes. The ground effect is neglected and the mass center and the body-fixed frame origin are assumed coincident. Moreover, only for controller synthesis purposes, the helicopter structure is assumed to be symmetrical, which results in a moment of inertia tensor with just diagonal inertia terms.

2.2. Helicopter Kinematics

The helicopter as a rigid body is characterized by a frame linked to it. Let $\mathcal{B} = \{\vec{x}_L, \vec{y}_L, \vec{z}_L\}$ be the body-fixed frame, where the \vec{x}_L axis is the helicopter normal flight direction, \vec{y}_L is orthogonal to \vec{x}_L and positive to starboard in the horizontal plane, whereas \vec{z}_L is oriented in ascendant sense and orthogonal to the plane $\vec{x}_L O \vec{y}_L$. The inertial frame $\mathcal{I} = \{\vec{x}, \vec{y}, \vec{z}\}$ is considered fixed with respect to the earth (see Fig. 1).

Let the vector $\xi = [x \ y \ z]'$ represent the position of the helicopter mass center expressed in the inertial frame

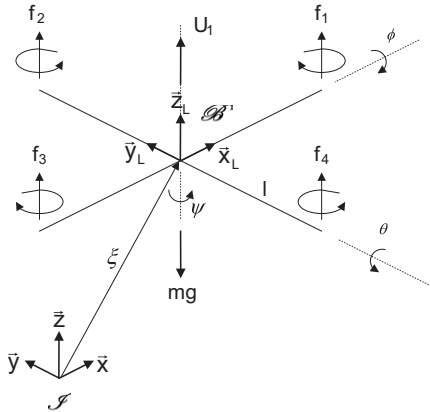


Fig. 1. Quadrotor helicopter scheme.

\mathcal{I} .¹ The vehicle orientation is given by a rotation matrix $\mathbf{R}_{\mathcal{I}} : \mathcal{B} \rightarrow \mathcal{I}$, where $\mathbf{R}_{\mathcal{I}} \in SO(3)$ is an orthonormal rotation matrix [10]. In this study, the XYZ fixed Euler angles have been used to describe the helicopter rotation matrix, $\mathbf{R}_{\mathcal{I}}$, with respect to the ground. These angles are bounded as follows: the roll angle, ϕ , by $(-\pi/2 < \phi < \pi/2)$, the pitch angle, θ , by $(-\pi/2 < \theta < \pi/2)$ and the yaw angle, ψ , by $(-\pi < \psi < \pi)$.

From these three rotations, the following rotation matrix from \mathcal{B} to \mathcal{I} is obtained:

$$\mathbf{R}_{\mathcal{I}} = \begin{bmatrix} C\psi C\theta & C\psi S\theta S\phi - S\psi C\phi & C\psi S\theta C\phi + S\psi S\phi \\ S\psi C\theta & S\psi S\theta S\phi + C\psi C\phi & S\psi S\theta C\phi - C\psi S\phi \\ -S\theta & C\theta S\phi & C\theta C\phi \end{bmatrix} \quad (1)$$

where $C \cdot = \cos(\cdot)$ and $S \cdot = \sin(\cdot)$.

The kinematic equations of the rotational and translational movements are obtained by means of the rotation matrix. The translational kinematic can be written as:

$$\mathbf{v}_{\mathcal{I}} = \mathbf{R}_{\mathcal{I}} \cdot \mathbf{v}_{\mathcal{B}} \quad (2)$$

where $\mathbf{v}_{\mathcal{I}} = [u_0 \ v_0 \ w_0]'$ and $\mathbf{v}_{\mathcal{B}} = [u_L \ v_L \ w_L]'$ are the linear velocities of the helicopter mass center expressed in the inertial frame and body-fixed frame, respectively.

The rotational kinematic can be obtained from the relationship between the rotation matrix and its derivative with an skew-symmetric matrix [24]. Thus, after some algebraic manipulations it can be posed as follows:

$$\dot{\boldsymbol{\eta}} = \mathbf{W}_{\boldsymbol{\eta}}^{-1} \boldsymbol{\omega}$$

$$\begin{bmatrix} \dot{\phi} \\ \dot{\theta} \\ \dot{\psi} \end{bmatrix} = \begin{bmatrix} 1 & \sin \phi \tan \theta & \cos \phi \tan \theta \\ 0 & \cos \phi & -\sin \phi \\ 0 & \sin \phi \sec \theta & \cos \phi \sec \theta \end{bmatrix} \begin{bmatrix} p \\ q \\ r \end{bmatrix} \quad (3)$$

where $\boldsymbol{\eta} = [\phi \ \theta \ \psi]'$, and $\boldsymbol{\omega} = [p \ q \ r]'$ is the angular velocity vector expressed in the body-fixed frame.

2.3. Lagrange-Euler Equations

The helicopter motion dynamic equations can be expressed by the Lagrange-Euler formalism based on the kinetic and potential energy concept:

$$\Gamma_i = \frac{d}{dt} \left(\frac{\partial L}{\partial \dot{q}_i} \right) - \frac{\partial L}{\partial q_i} \quad (4)$$

$$L = E_c - E_p$$

¹ The notation prime ' denotes transpose.

where L is the Lagrangian, E_c is the total kinetic energy, E_p is the total potential energy, q_i is the i -th generalized coordinate and Γ_i is the i -th generalized force/torque given by nonconservative forces/torques.

The generalized coordinates for a rigid body rotating in the three-dimensional space can be written as [5]:

$$\mathbf{q} = [x \ y \ z \ \phi \ \theta \ \psi]' \in \mathfrak{R}^6$$

The Lagrangian expression of the helicopter is given by:

$$L(\mathbf{q}, \dot{\mathbf{q}}) = E_{c_{Trans}} + E_{c_{Rot}} - E_p \quad (5)$$

where $E_{c_{Trans}}$ is the translational kinetic energy and $E_{c_{Rot}}$ is the rotational kinetic energy (see [27]).

The complete movement equation is obtained from the Lagrangian expression (5). However, since the Lagrangian does not contain kinetic energy terms combining $\dot{\xi}$ and $\dot{\eta}$, the Lagrange-Euler equations can be divided into translational and rotational dynamics and expressed as follows [27]:

$$m\ddot{\xi} + mg\mathbf{e}_3 = \mathbf{f}_\xi \quad (6)$$

$$\mathbf{M}(\eta)\ddot{\eta} + \mathbf{C}(\eta, \dot{\eta})\dot{\eta} = \boldsymbol{\tau}_\eta \quad (7)$$

where m is the helicopter mass, g is the gravitational acceleration, $\boldsymbol{\tau}_\eta \in \mathfrak{R}^3$ represents the roll, pitch and yaw moments, and $\mathbf{f}_\xi = \mathbf{R}_{\mathcal{J}}\hat{\mathbf{f}} + \boldsymbol{\alpha}_T$ is the translational forces vector. This translational force is divided into two parts: first the term $\mathbf{R}_{\mathcal{J}}\hat{\mathbf{f}}$ constitutes the applied force to the helicopter due to the main control input U_1 in the \bar{z} axis direction, being $\mathbf{R}_{\mathcal{J}}\hat{\mathbf{f}} = \mathbf{R}_{\mathcal{J}_{e_3}}U_1$.² The second part, $\boldsymbol{\alpha}_T = [A_x \ A_y \ A_z]'$, is the aerodynamic forces vector, whose components are in the \bar{x} , \bar{y} and \bar{z} axes, respectively. Aerodynamic forces are considered like external disturbances for the control design (more details can be found in [27]). $\mathbf{M}(\eta) = \mathbf{W}'_\eta \mathbf{J} \mathbf{W}_\eta$ represents the symmetric positive definite inertia matrix, where \mathbf{J} is the moment of inertia tensor, and is written as follows:

$$\mathbf{M}(\eta) =$$

$$\begin{bmatrix} I_{xx} & 0 & -I_{xx}S\theta \\ 0 & I_{yy}C^2\phi + I_{zz}S^2\phi & (I_{yy} - I_{zz})C\phi S\phi C\theta \\ -I_{xx}S\theta & (I_{yy} - I_{zz})C\phi S\phi C\theta & I_{xx}S^2\theta + I_{yy}S^2\phi C^2\theta + I_{zz}C^2\phi C^2\theta \end{bmatrix}$$

The Coriolis matrix is given by:

$$\mathbf{C}(\eta, \dot{\eta}) = \begin{bmatrix} c_{11} & c_{12} & c_{13} \\ c_{21} & c_{22} & c_{23} \\ c_{31} & c_{32} & c_{33} \end{bmatrix}$$

where

$$c_{11} = 0$$

$$c_{12} = (I_{yy} - I_{zz}) (\dot{\theta} C\phi S\phi + \dot{\psi} S^2\phi C\theta) \\ + (I_{zz} - I_{yy}) \dot{\psi} C^2\phi C\theta - I_{xx} \dot{\psi} C\theta$$

$$c_{13} = (I_{zz} - I_{yy}) \dot{\psi} C\phi S\phi C^2\theta$$

$$c_{21} = (I_{zz} - I_{yy}) (\dot{\theta} C\phi S\phi + \dot{\psi} S^2\phi C\theta) \\ + (I_{yy} - I_{zz}) \dot{\psi} C^2\phi C\theta + I_{xx} \dot{\psi} C\theta$$

$$c_{22} = (I_{zz} - I_{yy}) \dot{\phi} C\phi S\phi$$

$$c_{23} = -I_{xx} \dot{\psi} S\theta C\theta + I_{yy} \dot{\psi} S^2\phi C\theta S\theta + I_{zz} \dot{\psi} C^2\phi S\theta C\theta$$

$$c_{31} = (I_{yy} - I_{zz}) \dot{\psi} C^2\theta S\phi C\phi - I_{xx} \dot{\theta} C\theta$$

$$c_{32} = (I_{zz} - I_{yy}) (\dot{\theta} C\phi S\phi S\theta + \dot{\phi} S^2\phi C\theta) \\ + (I_{yy} - I_{zz}) \dot{\phi} C^2\phi C\theta + I_{xx} \dot{\psi} S\theta C\theta \\ - I_{yy} \dot{\psi} S^2\phi S\theta C\theta - I_{zz} \dot{\psi} C^2\phi S\theta C\theta$$

$$c_{33} = (I_{yy} - I_{zz}) \dot{\phi} C\phi S\phi C^2\theta - I_{yy} \dot{\theta} S^2\phi C\theta S\theta \\ - I_{zz} \dot{\theta} C^2\phi C\theta S\theta + I_{xx} \dot{\theta} C\theta S\theta$$

Hence, the mathematical model used for controller synthesis purposes that describes the helicopter translational movement computed from Eq. (6) can be written in the following form:

$$\begin{cases} \ddot{x} = \frac{1}{m} (\cos \psi \sin \theta \cos \phi + \sin \psi \sin \phi) U_1 + \frac{A_x}{m} \\ \ddot{y} = \frac{1}{m} (\sin \psi \sin \theta \cos \phi - \cos \psi \sin \phi) U_1 + \frac{A_y}{m} \\ \ddot{z} = -g + \frac{1}{m} (\cos \theta \cos \phi) U_1 + \frac{A_z}{m} \end{cases} \quad (8)$$

while the rotational dynamic Eq. (7) is given as follows:

$$\ddot{\eta} = \mathbf{M}(\eta)^{-1} (\boldsymbol{\tau}_\eta - \mathbf{C}(\eta, \dot{\eta})\dot{\eta}) \quad (9)$$

3. Control Scheme

The control strategy used in this study is based on the idea presented in Fig. 2, which is composed by an outer-inner control structure. To solve the path tracking problem for an unmanned aerial vehicle (in this case, a quadrotor helicopter) two control techniques are proposed. These techniques are designed to guide the vehicle even if parametric and structural uncertainties are considered, and also

² The notation \mathbf{e}_3 represents the vector $\mathbf{e}_3 = [0 \ 0 \ 1]'$. Thus, the term $\mathbf{R}_{\mathcal{J}_{e_3}}$ denotes the third column of the rotation matrix.

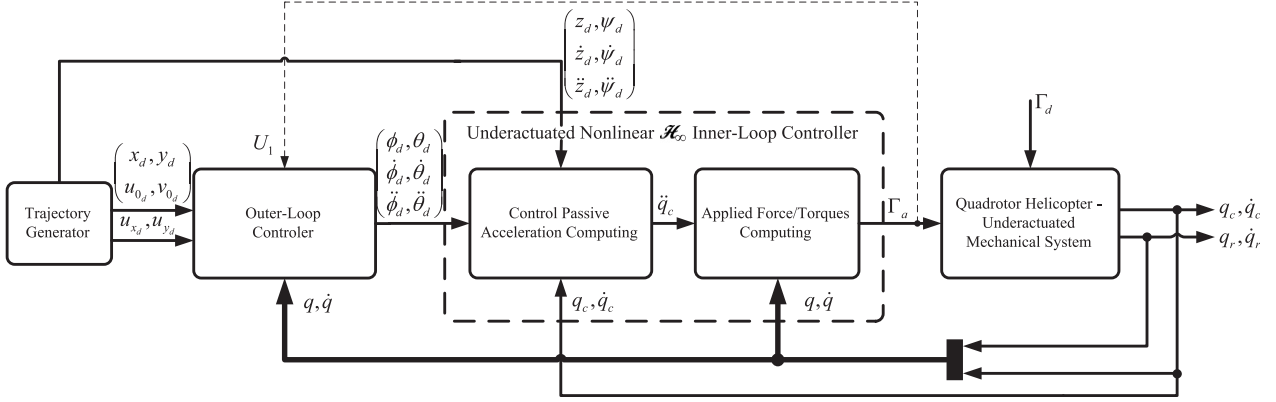


Fig. 2. Nonlinear \mathcal{H}_∞ control block diagram for the underactuated quadrotor helicopter with an outer-loop controller. (Thick and thin lines mean full and partial data vectors, respectively. Dashed line means a single data.)

when sustained disturbances affect on all the degrees of freedom of the helicopter.

The path to be followed in the \mathfrak{R}^3 Cartesian space is generated beforehand by the *Trajectory Generator* block. To compute the reference trajectory, a virtual reference vehicle with the same quadrotor mathematical model defined in Section 2 is used. However, the trajectory is generated under the assumption that there are no external disturbances affecting the system, and its attitude is in steady-state. Firstly, considering that the vehicle is hovering, the desired altitude, z_d , its time derivatives and the desired thrust, U_{1d} , are computed using model (8). These altitude references, jointly with the desired yaw angle, ψ_d , and its time derivatives, are supplied by the *Trajectory Generator* block to the inner-loop controller through a feedforward action. The yaw reference angle is defined separately. In a second step, making use of the computed reference thrust, U_{1d} , the same block generates the xy reference trajectory, being these reference positions, x_d and y_d , their speeds and the virtual control references, u_{x_d} and u_{y_d} (see definition in Section 5), provided to the outer-loop controller.

A state-space predictive controller to control the movements in the xy plane is executed in the *Outer-Loop Controller* block. This predictive controller is based on the xy error model between the helicopter mathematical model and the virtual reference one. Moreover, the integral of the position error is considered to be part of the state vector, which makes the sustained disturbances rejection possible. From the virtual control actions, u_x^c and u_y^c (see Eq. (46)), calculated by this controller, the desired roll, ϕ_d , and pitch, θ_d , angles are computed.

Keeping in mind that the quadrotor helicopter is an underactuated mechanical system, a nonlinear \mathcal{H}_∞ controller designed for this kind of systems is used in the inner-loop control law. The synthesized controller considers the overall dynamic behavior in order to control the helicopter attitude, ϕ , θ and ψ , and the altitude, z .

Furthermore, this control law also includes the integral of both the altitude and the angular position error in the state vector in order to obtain null steady-state error in presence of sustained disturbances. The underactuated nonlinear \mathcal{H}_∞ controller is split up into two parts: first the controlled coordinates accelerations required to track the desired reference are computed; in a second step, these values are considered to generate the forces and torques applied to the quadrotor helicopter, $\Gamma_a = [U_1 \tau_{\phi_a} \tau_{\theta_a} \tau_{\psi_a}]'$.

Taking into account the cascade structure of this strategy and considering the performance attained by the inner-loop controller, the quadrotor helicopter is assumed stabilized at the desired height. Therefore, for the design of the outer-loop controller, the thrust, U_1 , and the Euler angles can be considered as time-varying parameters, and in steady-state between two outer-loop sampling time.

In the following sections, both the inner-loop and the outer-loop controllers will be presented.

4. Inner-loop Controller

In this section the height and the rotational subsystem control law to achieve robustness in presence of sustained disturbances and parametric uncertainty is developed. A nonlinear \mathcal{H}_∞ controller, designed for underactuated mechanical systems, is proposed to carry out this task.

As stated at the introduction of the study, the helicopter dynamic model represents an underactuated mechanical system [10] since there are more degrees of freedom than actuators. The dynamic equations of this kind of system with n DOF can be partitioned into two components, one corresponding to the passive generalized coordinates, $\mathbf{q}_p \in \mathfrak{R}^{n_p}$, and the other to the active ones, $\mathbf{q}_a \in \mathfrak{R}^{n_a}$, where $n = n_p + n_a$.

It is well-known that no more than n_a degrees of freedom can be controlled at each moment by the external generalized forces/torques [33]. Therefore, the n_a DOF to

be controlled should be grouped in a vector $\mathbf{q}_c \in \mathfrak{R}^{n_a}$, while the remaining generalized coordinates should be grouped in a vector $\mathbf{q}_r \in \mathfrak{R}^{n-n_a}$. Whenever there is a coupling between the passive and active dynamics, the passive degrees of freedom can be chosen to be controlled using this feature (e.g. [26]). In this study, the controlled degrees of freedom vector is chosen the same as the active one while the remaining coordinates vector is selected as the passive one. Accordingly, the passive and active notations are maintained, and for the case of the quadrotor helicopter, $\mathbf{q}_p = [x \ y]'$ and $\mathbf{q}_a = [z \ \phi \ \theta \ \psi]'$. As stated before, the advantage of this method is based on the knowledge of all underactuated system's behaviour at the moment to compute the control signals, and not solely considering the remaining coordinates' behaviour as external disturbances.

Thus, the quadrotor dynamic equations (6) and (7) can be written in the following form:

$$\begin{aligned} \begin{bmatrix} \mathbf{\Gamma}_p + \delta_p \\ \mathbf{\Gamma}_a + \delta_a \end{bmatrix} &= \begin{bmatrix} \mathbf{I}_{pp}(\mathbf{q}) & \mathbf{I}_{pa}(\mathbf{q}) \\ \mathbf{I}_{ap}(\mathbf{q}) & \mathbf{I}_{aa}(\mathbf{q}) \end{bmatrix} \begin{bmatrix} \ddot{\mathbf{q}}_p \\ \ddot{\mathbf{q}}_a \end{bmatrix} \\ &+ \begin{bmatrix} \mathbf{C}_{pp}(\mathbf{q}, \dot{\mathbf{q}}) & \mathbf{C}_{pa}(\mathbf{q}, \dot{\mathbf{q}}) \\ \mathbf{C}_{ap}(\mathbf{q}, \dot{\mathbf{q}}) & \mathbf{C}_{aa}(\mathbf{q}, \dot{\mathbf{q}}) \end{bmatrix} \begin{bmatrix} \dot{\mathbf{q}}_p \\ \dot{\mathbf{q}}_a \end{bmatrix} + \begin{bmatrix} \mathbf{G}_p(\mathbf{q}) \\ \mathbf{G}_a(\mathbf{q}) \end{bmatrix} \end{aligned} \quad (10)$$

where

$$\mathbf{I}_{pp} = \begin{bmatrix} mC\psi C\theta & mS\psi C\theta \\ m(C\psi S\theta S\phi - S\psi C\phi) & m(S\psi S\theta S\phi + C\psi C\phi) \end{bmatrix}$$

$$\mathbf{I}_{pa} = \begin{bmatrix} -mS\theta & \mathbb{O}_{1 \times 3} \\ mC\theta S\phi & \mathbb{O}_{1 \times 3} \end{bmatrix}$$

$$\mathbf{I}_{ap} = \begin{bmatrix} m(C\psi S\theta C\phi + S\psi S\phi) & m(S\psi S\theta C\phi - C\psi S\phi) \\ \mathbb{O}_{3 \times 1} & \mathbb{O}_{3 \times 1} \end{bmatrix}$$

$$\mathbf{I}_{aa} = \begin{bmatrix} mC\theta C\phi & \mathbb{O}_{1 \times 3} \\ \mathbb{O}_{3 \times 1} & \mathbf{M}(\boldsymbol{\eta}) \end{bmatrix}$$

$$\mathbf{C}_{pp} = \mathbb{O}_{2 \times 2}; \quad \mathbf{C}_{pa} = \mathbb{O}_{2 \times 4}; \quad \mathbf{C}_{ap} = \mathbb{O}_{4 \times 2};$$

$$\mathbf{C}_{aa} = \begin{bmatrix} 0 & \mathbb{O}_{1 \times 3} \\ \mathbb{O}_{3 \times 1} & \mathbf{C}(\boldsymbol{\eta}, \dot{\boldsymbol{\eta}}) \end{bmatrix}$$

$$\mathbf{G}_p = \begin{bmatrix} -mgS\theta \\ mgC\theta S\phi \end{bmatrix}, \quad \mathbf{G}_a = \begin{bmatrix} mgC\theta C\phi \\ \mathbb{O}_{3 \times 1} \end{bmatrix}$$

$$\begin{aligned} \delta_p &= -(\Delta \mathbf{I}_{pp}(\mathbf{q})\ddot{\mathbf{q}}_p + \Delta \mathbf{I}_{pa}(\mathbf{q})\ddot{\mathbf{q}}_a + \Delta \mathbf{C}_{pp}(\mathbf{q}, \dot{\mathbf{q}})\dot{\mathbf{q}}_p \\ &\quad + \Delta \mathbf{C}_{pa}(\mathbf{q}, \dot{\mathbf{q}})\dot{\mathbf{q}}_a + \Delta \mathbf{G}_p(\mathbf{q}) - \mathbf{\Gamma}_{d_p}) \end{aligned}$$

$$\begin{aligned} \delta_a &= -(\Delta \mathbf{I}_{ap}(\mathbf{q})\ddot{\mathbf{q}}_p + \Delta \mathbf{I}_{aa}(\mathbf{q})\ddot{\mathbf{q}}_a + \Delta \mathbf{C}_{ap}(\mathbf{q}, \dot{\mathbf{q}})\dot{\mathbf{q}}_p \\ &\quad + \Delta \mathbf{C}_{aa}(\mathbf{q}, \dot{\mathbf{q}})\dot{\mathbf{q}}_a + \Delta \mathbf{G}_a(\mathbf{q}) - \mathbf{\Gamma}_{d_a}) \end{aligned}$$

$\mathbf{\Gamma}_p \in \mathfrak{R}^{n_p}$ and $\mathbf{\Gamma}_a \in \mathfrak{R}^{n_a}$ are the forces/torques in the passive and active DOFs, respectively. In the case of the quadrotor helicopter, $\mathbf{\Gamma}_p = [0 \ 0]'$ and $\mathbf{\Gamma}_a = [U_1 \ \tau_{\phi_a} \ \tau_{\theta_a} \ \tau_{\psi_a}]'$. δ_p and δ_a represent the total effect of the parametric uncertainties (matrices expressed by $\Delta \bullet$) and energy-bounded external disturbances on the passive, $\mathbf{\Gamma}_{d_p}$, and active, $\mathbf{\Gamma}_{d_a}$, DOF, respectively.

Taking into account this partition and from the second row of (10):

$$\begin{aligned} \mathbf{\Gamma}_a + \delta_a &= \mathbf{I}_{ap}(\mathbf{q})\ddot{\mathbf{q}}_p + \mathbf{I}_{aa}(\mathbf{q})\ddot{\mathbf{q}}_a + \mathbf{C}_{ap}(\mathbf{q}, \dot{\mathbf{q}})\dot{\mathbf{q}}_p \\ &\quad + \mathbf{C}_{aa}(\mathbf{q}, \dot{\mathbf{q}})\dot{\mathbf{q}}_a + \mathbf{G}_a(\mathbf{q}) \end{aligned} \quad (11)$$

the controlled degrees of freedom acceleration (in this case, the active ones) can be isolated, yielding [33]:

$$\ddot{\mathbf{q}}_a = -\mathbf{I}_{aa}^{-1}(\mathbf{q})(\mathbf{C}_{aa}(\mathbf{q}, \dot{\mathbf{q}})\dot{\mathbf{q}}_a + \mathbf{G}_a(\mathbf{q}) - \bar{\mathbf{\Gamma}} - \delta_a) \quad (12)$$

where $\bar{\mathbf{\Gamma}} = \mathbf{\Gamma}_a - \mathbf{I}_{ap}(\mathbf{q})\ddot{\mathbf{q}}_p - \mathbf{C}_{ap}(\mathbf{q}, \dot{\mathbf{q}})\dot{\mathbf{q}}_p$.

By defining the tracking error vector of the active DOFs as follows [26]:

$$\mathbf{x}_a = \begin{bmatrix} \dot{\tilde{\mathbf{q}}}_a \\ \tilde{\mathbf{q}}_a \\ \int \tilde{\mathbf{q}}_a dt \end{bmatrix} = \begin{bmatrix} \dot{\mathbf{q}}_a - \dot{\mathbf{q}}_a^d \\ \mathbf{q}_a - \mathbf{q}_a^d \\ \int (\mathbf{q}_a - \mathbf{q}_a^d) dt \end{bmatrix} \quad (13)$$

Equation (12) can be written in the state space form:

$$\dot{\mathbf{x}}_a = \bar{\mathbf{f}}(\mathbf{x}_a, t) + \bar{\mathbf{g}}_0(\mathbf{q}, \dot{\mathbf{q}}, \ddot{\mathbf{q}}_a^d, \dot{\mathbf{q}}_a^d) + \bar{\mathbf{g}}(\mathbf{x}_a, t)\bar{\mathbf{\Gamma}} + \bar{\mathbf{k}}(\mathbf{x}_a, t)\delta_a, \quad (14)$$

where

$$\bar{\mathbf{f}}(\mathbf{x}_a, t) = \begin{bmatrix} -\mathbf{I}_{aa}^{-1}\mathbf{C}_{aa} & \mathbb{O} & \mathbb{O} \\ \mathbb{1} & \mathbb{O} & \mathbb{O} \\ \mathbb{O} & \mathbb{1} & \mathbb{O} \end{bmatrix} \mathbf{x}_a,$$

$$\bar{\mathbf{g}}_0(\mathbf{q}, \dot{\mathbf{q}}, \ddot{\mathbf{q}}_a^d, \dot{\mathbf{q}}_a^d) = \begin{bmatrix} -\mathbf{I}_{aa}^{-1}(\mathbf{I}_{aa}\ddot{\mathbf{q}}_a^d + \mathbf{C}_{aa}\dot{\mathbf{q}}_a^d + \mathbf{G}_a) \\ \mathbb{O} \\ \mathbb{O} \end{bmatrix},$$

$$\bar{\mathbf{g}}(\mathbf{x}_a, t) = \bar{\mathbf{k}}(\mathbf{x}_a, t) = \begin{bmatrix} \mathbf{I}_{aa}^{-1} \\ \mathbb{O} \\ \mathbb{O} \end{bmatrix},$$

where \mathbf{q}_a^d , $\dot{\mathbf{q}}_a^d$ and $\ddot{\mathbf{q}}_a^d \in \mathfrak{R}^{n_a}$ are the desired trajectory and the corresponding velocity and acceleration, respectively. $\mathbb{1}$ is the identity matrix and \mathbb{O} the zero matrix, both of n_a -th order. Note that an integral term has been included in the error vector. This term will allow the achievement of a null steady-state error when persistent disturbances are acting on the system [26].

4.1. Nonlinear \mathcal{H}_∞ Controller Design

The nonlinear \mathcal{H}_∞ controller used to the inner-loop considers the overall helicopter dynamic behavior.

As a previous step to synthesize the control law, the following state transformation is used:

$$z = \begin{bmatrix} z_1 \\ z_2 \\ z_3 \end{bmatrix} = T_o x_a = \begin{bmatrix} T_1 & T_2 & T_3 \\ \mathbb{0} & \mathbb{1} & \mathbb{1} \\ \mathbb{0} & \mathbb{0} & \mathbb{1} \end{bmatrix} \begin{bmatrix} \dot{\tilde{q}}_a \\ \tilde{q}_a \\ \int \tilde{q}_a dt \end{bmatrix} \quad (15)$$

with $T_1 = \rho \mathbb{1}$, where ρ is a positive scalar and $\mathbb{1} \in \mathfrak{N}^{n_a \times n_a}$ is the identity matrix.

Equation (14) can be rewritten as follows [33]:

$$\dot{x}_a = f(x_a, t) + g(x_a, t)T_1(-F(x_e) + \bar{\Gamma}) + k(x_a, t)d, \quad (16)$$

$f(x_a, t) =$

$$T_o^{-1} \begin{bmatrix} -I_{aa}^{-1} C_{aa} & \mathbb{0} & \mathbb{0} \\ T_1^{-1} & \mathbb{1} - T_1^{-1} T_2 & -\mathbb{1} + T_1^{-1} (T_2 - T_3) \\ \mathbb{0} & \mathbb{1} & -\mathbb{1} \end{bmatrix} T_o x_a,$$

$$g(x_a, t) = k(x_a, t) = T_o^{-1} \begin{bmatrix} I_{aa}^{-1} \\ \mathbb{0} \\ \mathbb{0} \end{bmatrix},$$

$$F(x_e) = I_{aa}(\ddot{q}_a^d - T_1^{-1} T_2 \dot{\tilde{q}}_a - T_1^{-1} T_3 \tilde{q}_a) + C_{aa} \left(\dot{q}_a^d - T_1^{-1} T_2 \tilde{q}_a - T_1^{-1} T_3 \int \tilde{q}_a dt \right) + G_a$$

where $d = \rho \mathbb{1} \delta_a \in \mathfrak{N}^{n_a}$ is the vector of external disturbances.

The following control law is proposed for the controlled subsystem:

$$\begin{aligned} \bar{\Gamma} &= I_{aa}(q) \ddot{q}_a + C_{aa}(q, \dot{q}) \dot{q}_a + G_a(q) \\ &\quad - T_1^{-1} (I_{aa} T \dot{x}_a + C_{aa} T x_a) + T_1^{-1} u \end{aligned} \quad (17)$$

where matrix T can be partitioned as follows:

$$T = [T_1 \quad T_2 \quad T_3].$$

This proposed control law can be split up into three different parts: the first one consists of the first three terms of that equation, which are designed in order to counter the effects of the system dynamics (12). The second part consists of terms including the error vector x_a and its derivative, \dot{x}_a . Assuming $\delta_a \equiv 0$, these two terms of the control law enable perfect tracking, which means that they represent the *essential control* effort needed to perform the task. Finally, the third part includes vector u , which represents the *additional control* effort needed for disturbance rejection.

It can be pointed out that, despite the preceding control law might not seem a well posed system, it will be shown afterwards that the computed forces/torques does not rely on DOF accelerations, but on their references. In this way, the *control acceleration* \ddot{q}_a , computed in Eq. (27), is replaced into (17) which makes it a well posed equation.

Substituting the expression of the control law from (17) into the system (12) one gets:

$$I_{aa}(q) T \dot{x}_a + C_{aa}(q, \dot{q}) T x_a = u + d \quad (18)$$

This expression is the same of the system (16) when $u = T_1(-F(x_e) + \bar{\Gamma})$, and represents the *dynamic equation of the system error*. Therefore, Eq. (16) considering the *additional control* input vector u is used to apply the nonlinear \mathcal{H}_∞ theoretical results presented in [36]. This *additional control* signal provides \mathcal{H}_∞ robustness and represents a state feedback.

The performance of the controlled system can be derived from the following cost variable $\zeta \in \mathfrak{N}^{2n_a}$:

$$\zeta = W \begin{bmatrix} h(x_a) \\ u \end{bmatrix}, \quad (19)$$

where $h(x_a) \in \mathfrak{N}^{n_a}$ represents a function of the vector of states to be controlled, and $W \in \mathfrak{N}^{2n_a \times 2n_a}$ is a weighting matrix.

Taking into account the nonlinear Eq. (18) and the above-defined cost variable (19), if the states x_a are assumed to be available for measurement, then the nonlinear \mathcal{H}_∞ control problem can be posed as follows [36]:

“Find the smallest value $\gamma^* \geq 0$ such that for any $\gamma \geq \gamma^*$ exists an additional control effort $u = u(x_a, t)$, such that the L_2 gain from the disturbance signals d to the cost variable $\zeta = W [h'(x_a) \quad u']^T$ is less than or equal to a given attenuation level γ , that is:”.

$$\int_0^T \|\zeta\|_2^2 dt \leq \gamma^2 \int_0^T \|d\|_2^2 dt. \quad (20)$$

The internal term of the integral expression on the left-hand side of inequality (20) can be written as:

$$\|\zeta\|_2^2 = \zeta' \zeta = [h'(x_a) \quad u'] W' W \begin{bmatrix} h(x_a) \\ u \end{bmatrix}$$

and the symmetric positive definite matrix $W'W$ can be partitioned as follows:

$$W'W = \begin{bmatrix} Q & S \\ S' & R \end{bmatrix} \quad (21)$$

Matrices Q and R are symmetric positive definite and the fact that $W'W > \mathbb{0}$ guarantees that $Q - SR^{-1}S' > \mathbb{0}$, where $\mathbb{0}$ is the n_a -th order zero matrix.

Taking into account the definition of the error vector, \mathbf{x}_a , and the definition of the cost variable, ζ , the following structures are considered for matrices \mathbf{Q} and \mathbf{S} in (21):

$$\mathbf{Q} = \begin{bmatrix} \mathbf{Q}_1 & \mathbf{Q}_{12} & \mathbf{Q}_{13} \\ \mathbf{Q}_{12} & \mathbf{Q}_2 & \mathbf{Q}_{23} \\ \mathbf{Q}_{13} & \mathbf{Q}_{23} & \mathbf{Q}_3 \end{bmatrix}, \quad \mathbf{S} = \begin{bmatrix} \mathbf{S}_1 \\ \mathbf{S}_2 \\ \mathbf{S}_3 \end{bmatrix}.$$

Under these assumptions, an optimal state feedback *additional control* effort $\mathbf{u}^*(\mathbf{x}_a, t)$ can be computed if a smooth solution $V(\mathbf{x}_a, t)$, with $\mathbf{x}_{a0} = 0$ and $V(\mathbf{x}_{a0}, t) \equiv 0$ for $t \geq 0$, is found for the following HJBI equation [37]:

$$\begin{aligned} \frac{\partial V}{\partial t} + \frac{\partial V}{\partial \mathbf{x}_a} f(\mathbf{x}_a, t) + \frac{1}{2} \frac{\partial V}{\partial \mathbf{x}_a} \left[\frac{1}{\gamma^2} k(\mathbf{x}_a, t) k'(\mathbf{x}_a, t) \right. \\ \left. - g(\mathbf{x}_a, t) \mathbf{R}^{-1} g'(\mathbf{x}_a, t) \right] \frac{\partial V}{\partial \mathbf{x}_a} - \frac{\partial V}{\partial \mathbf{x}_a} g(\mathbf{x}_a, t) \mathbf{R}^{-1} \mathbf{S}' h(\mathbf{x}_a) \\ + \frac{1}{2} h'(\mathbf{x}_a) (\mathbf{Q} - \mathbf{S} \mathbf{R}^{-1} \mathbf{S}') h(\mathbf{x}_a) = 0 \end{aligned} \quad (22)$$

for each $\gamma > \sqrt{\sigma_{\max}(\mathbf{R})} \geq 0$, where σ_{\max} stands for the maximum singular value. In such a case, the optimal state feedback *additional control* effort is derived as (see [11]):

$$\mathbf{u}^* = -\mathbf{R}^{-1} \left(\mathbf{S}' h(\mathbf{x}_a) + g'(\mathbf{x}_a, t) \frac{\partial V(\mathbf{x}_a, t)}{\partial \mathbf{x}_a} \right). \quad (23)$$

As stated before, the solution of the HJBI equation depends on the choice of the cost variable, ζ , and particularly on the selection of function $h(\mathbf{x}_a)$. In this study, this function is taken to be equal to the error vector, that is, $h(\mathbf{x}_a) = \mathbf{x}_a$. Once this function has been selected, computing the *additional control* effort, \mathbf{u} , will require finding the solution, $V(\mathbf{x}_a, t)$, to the HJBI equation posed in [11]. The details of how this solution is achieved can be found in [25]. The following theorem will help do this.

Theorem: Let $V(\mathbf{x}_a, t)$ be the parameterized scalar function:

$$V(\mathbf{x}_a, t) = \frac{1}{2} \mathbf{x}_a' \mathbf{T}_o' \begin{bmatrix} \mathbf{I}_{aa} & \mathbf{0} & \mathbf{0} \\ \mathbf{0} & \mathbf{Y} & \mathbf{X} - \mathbf{Y} \\ \mathbf{0} & \mathbf{X} - \mathbf{Y} & \mathbf{Z} + \mathbf{Y} \end{bmatrix} \mathbf{T}_o \mathbf{x}_a, \quad (24)$$

where \mathbf{X} , \mathbf{Y} and $\mathbf{Z} \in \mathfrak{R}^{n_a \times n_a}$ are constant, symmetric, and positive definite matrices such that $\mathbf{Z} - \mathbf{X} \mathbf{Y}^{-1} \mathbf{X} + 2\mathbf{X} > \mathbf{0}$, and \mathbf{T}_o is as defined in (15). Let \mathbf{T} be the matrix

appearing in (17). If these matrices verify the following equation:

$$\begin{aligned} \begin{bmatrix} \mathbf{0} & \mathbf{Y} & \mathbf{X} \\ \mathbf{Y} & 2\mathbf{X} & \mathbf{Z} + 2\mathbf{X} \\ \mathbf{X} & \mathbf{Z} + 2\mathbf{X} & \mathbf{0} \end{bmatrix} + \mathbf{Q} + \frac{1}{\gamma^2} \mathbf{T}' \mathbf{T} \\ - (\mathbf{S}' + \mathbf{T})' \mathbf{R}^{-1} (\mathbf{S}' + \mathbf{T}) = \mathbf{0} \end{aligned} \quad (25)$$

then, function $V(\mathbf{x}_a, t)$ constitutes a solution to the HJBI, for a sufficiently high value of γ .

The proof of this theorem can be found in [25]. \diamond

Once matrix \mathbf{T} is computed by solving some Riccati algebraic equations, substituting $V(\mathbf{x}_a, t)$ into the optimal state feedback *additional control* effort (23), the *additional control* effort \mathbf{u}^* corresponding to the \mathcal{H}_∞ optimal index γ is given by

$$\mathbf{u}^* = -\mathbf{R}^{-1} (\mathbf{S}' + \mathbf{T}) \mathbf{x}_a \quad (26)$$

Finally, if the *additional control* effort (26) is replaced into (18) under the assumption that $\mathbf{d} = 0$, and after some manipulations, the *control acceleration* for the controlled subsystem can be obtained as:

$$\ddot{\mathbf{q}}_a = \ddot{\mathbf{q}}_a^d - \mathbf{K}_D \dot{\mathbf{q}}_a - \mathbf{K}_P \tilde{\mathbf{q}}_a - \mathbf{K}_I \int \tilde{\mathbf{q}}_a dt \quad (27)$$

where

$$\begin{aligned} \mathbf{K}_D &= \mathbf{T}_1^{-1} (\mathbf{T}_2 + \mathbf{I}_{aa}^{-1} \mathbf{C}_{aa} \mathbf{T}_1 + \mathbf{I}_{aa}^{-1} \mathbf{R}^{-1} (\mathbf{S}'_1 + \mathbf{T}_1)) \\ \mathbf{K}_P &= \mathbf{T}_1^{-1} (\mathbf{T}_3 + \mathbf{I}_{aa}^{-1} \mathbf{C}_{aa} \mathbf{T}_2 + \mathbf{I}_{aa}^{-1} \mathbf{R}^{-1} (\mathbf{S}'_2 + \mathbf{T}_2)) \\ \mathbf{K}_I &= -\mathbf{T}_1^{-1} (\mathbf{I}_{aa}^{-1} \mathbf{C}_{aa} \mathbf{T}_3 + \mathbf{I}_{aa}^{-1} \mathbf{R}^{-1} (\mathbf{S}'_3 + \mathbf{T}_3)) \end{aligned}$$

A particular case can be obtained when the components of weighting compound $\mathbf{W}'\mathbf{W}$ verify:

$$\mathbf{Q} = \begin{bmatrix} \omega_1^2 \mathbf{1} & \mathbf{0} & \mathbf{0} \\ \mathbf{0} & \omega_2^2 \mathbf{1} & \mathbf{0} \\ \mathbf{0} & \mathbf{0} & \omega_3^2 \mathbf{1} \end{bmatrix}, \quad \mathbf{S} = \begin{bmatrix} \mathbf{0} \\ \mathbf{0} \\ \mathbf{0} \end{bmatrix}, \quad \mathbf{R} = \omega_u^2 \mathbf{1}. \quad (28)$$

In this case, the following analytical expressions for the gain matrices have been obtained:

$$\begin{aligned} \mathbf{K}_D &= \frac{\sqrt{\omega_2^2 + 2\omega_1\omega_3}}{\omega_1} \mathbf{1} + \mathbf{I}_{aa}^{-1} \left(\mathbf{C}_{aa} + \frac{1}{\omega_u^2} \mathbf{1} \right), \\ \mathbf{K}_P &= \frac{\omega_3}{\omega_1} \mathbf{1} + \frac{\sqrt{\omega_2^2 + 2\omega_1\omega_3}}{\omega_1} \mathbf{I}_{aa}^{-1} \left(\mathbf{C}_{aa} + \frac{1}{\omega_u^2} \mathbf{1} \right), \\ \mathbf{K}_I &= \frac{\omega_3}{\omega_1} \mathbf{I}_{aa}^{-1} \left(\mathbf{C}_{aa} + \frac{1}{\omega_u^2} \mathbf{1} \right). \end{aligned}$$

where the parameters ω_1 , ω_2 , ω_3 and ω_u are tuned by a systematic procedure taking in mind a linear PID control action interpretation (see [19]).

Equation (27) gives the controlled degrees of freedom acceleration required to track the desired reference. The forces/torques in the active DOF can be computed using this *control acceleration*, which does not depend on the acceleration of the DOF controlled, but on their acceleration references as pointed out before. Thereby, as the control actions for the active degrees of freedom are the same as the controlled ones, the forces/torques applied to the quadrotor helicopter can be obtained by isolating vector $\ddot{\mathbf{q}}_p$ in the first row of (10) and replacing it in the second one, as follows:

$$\begin{aligned} \Gamma_a &= (\mathbf{I}_{aa}(\mathbf{q}) - \mathbf{I}_{ap}(\mathbf{q})\mathbf{I}_{pp}^{-1}\mathbf{I}_{pa})\ddot{\mathbf{q}}_a + \mathbf{b}_a(\mathbf{q}, \dot{\mathbf{q}}) \\ &\quad - \mathbf{I}_{ap}(\mathbf{q})\mathbf{I}_{pp}^{-1}\mathbf{b}_p(\mathbf{q}, \dot{\mathbf{q}}) \end{aligned} \quad (29)$$

where

$$\begin{aligned} \mathbf{b}_a(\mathbf{q}, \dot{\mathbf{q}}) &= \mathbf{C}_{aa}(\mathbf{q}, \dot{\mathbf{q}})\dot{\mathbf{q}}_a + \mathbf{C}_{ap}(\mathbf{q}, \dot{\mathbf{q}})\dot{\mathbf{q}}_p + \mathbf{G}_a(\mathbf{q}) \\ \mathbf{b}_p(\mathbf{q}, \dot{\mathbf{q}}) &= \mathbf{C}_{pa}(\mathbf{q}, \dot{\mathbf{q}})\dot{\mathbf{q}}_a + \mathbf{C}_{pp}(\mathbf{q}, \dot{\mathbf{q}})\dot{\mathbf{q}}_p + \mathbf{G}_p(\mathbf{q}) \end{aligned}$$

The proposed control law guarantees that all equilibrium points in the workspace are globally asymptotically stable for the controlled subsystem if the passive degrees of freedom are stable or converge asymptotically to the path to be followed. Therefore, the attraction basin in the inner closed-loop is enlarged or reduced by modifying the gains parameters. Meanwhile, the estimated attraction basin can be augmented by modifying the relation of gains between the inner-loop controller and outer-loop one, which guarantees convergence.

5. Outer-loop Controller

In this section a control law able to solve the path tracking problem on the xy plane is designed. A linear state-space MPC strategy based on the error model is used to perform that task.

The proposed control law is derived from the system (8), where only the equations describing the xy motion are used:

$$\begin{cases} \ddot{x} = \frac{1}{m}(\cos \psi \sin \theta \cos \phi + \sin \psi \sin \phi)U_1 + \frac{A_x}{m} \\ \ddot{y} = \frac{1}{m}(\sin \psi \sin \theta \cos \phi - \cos \psi \sin \phi)U_1 + \frac{A_y}{m} \end{cases} \quad (30)$$

The objective of this approach is to obtain a linear control law that leads the error between a real vehicle and a virtual reference one to zero. To obtain the error

model for the controller design, the system (30) is rewritten in a state-space form as $\dot{\hat{\mathbf{x}}}(t) = f(\hat{\mathbf{x}}(t), \hat{\mathbf{u}}(t))$, where $\hat{\mathbf{x}}(t) = [x(t) \ u_0(t) \ y(t) \ v_0(t)]'$ and $\hat{\mathbf{u}}(t) = [u_x(t) \ u_y(t)]'$ stand for the state-space and the virtual input vectors of the system, respectively. Since the aerodynamic forces, A_x and A_y , are assumed as external disturbances, they are not considered at the control design stage.

From (30) and the new state-space vectors, the system dynamic equation for the controller design can be written in the following form:

$$\dot{\hat{\mathbf{x}}}(t) = f(\hat{\mathbf{x}}(t), \hat{\mathbf{u}}(t)) = \begin{bmatrix} u_0(t) \\ u_x(t) \frac{U_1(t)}{m} \\ v_0(t) \\ u_y(t) \frac{U_1(t)}{m} \end{bmatrix} \quad (31)$$

with:

$$\begin{aligned} u_x(t) &\triangleq \cos \psi(t) \sin \theta(t) \cos \phi(t) + \sin \psi(t) \sin \phi(t) \\ u_y(t) &\triangleq \sin \psi(t) \sin \theta(t) \cos \phi(t) - \cos \psi(t) \sin \phi(t). \end{aligned} \quad (32)$$

Furthermore, system (30) show that the movement through the x and y axes depends on the control input U_1 . In fact, U_1 is the designed total thrust magnitude to obtain the desired linear movement, while u_x and u_y can be considered as the directions of U_1 that cause the movement through the x and y axes, respectively. As the input control $U_1(t)$ is computed by the inner-loop controller, which has a faster settling time than the outer one, for the outer-loop controller synthesis, this control action is considered as a time variant parameter to the x and y motions in (31). That is, between each outer-loop sampling time the inner-loop controlled variables are considered in steady-state.

Therefore, Eq. (32) is a definition of the system to be controlled, and through the virtual inputs, $u_x(t)$ and $u_y(t)$, the necessary values of ϕ and θ to guide the helicopter in the xy plane could be computed. However, these values can not be set directly since these angles are two of the outputs of the rotational subsystem; being the nonlinear \mathcal{H}_∞ inner-loop in charge of carrying out this task. On the other hand, assuming the error vector definition (13), Eq. (32) can be written as follows:

$$\begin{aligned} u_x(t) &\triangleq \cos(\psi) \sin(\tilde{\theta} + \theta_d) \cos(\tilde{\phi} + \phi_d) \\ &\quad + \sin(\psi) \sin(\tilde{\phi} + \phi_d) \\ u_y(t) &\triangleq \sin(\psi) \sin(\tilde{\theta} + \theta_d) \cos(\tilde{\phi} + \phi_d) \\ &\quad - \cos(\psi) \sin(\tilde{\phi} + \phi_d). \end{aligned} \quad (33)$$

Moreover, because of the cascade structure of the strategy proposed in this study (see Fig. 2), and considering

the closed-loop performance achieved by the inner-loop controller, the Euler angles error can be considered at the origin for the outer-loop controller design. Besides, it can be pointed out that the yaw angle, ψ , is assumed measurable for the computation of the desired magnitudes θ_d and ϕ_d . For this reason, the variable ψ_d has not been considered in Eq. (33). In consequence of these assumptions, the desired virtual directions vector, $\mathbf{u}_{xy}^d(k) = [u_x^d \ u_y^d]'$, to follow the path reference in the xy plane, is defined as follows:

$$\begin{aligned} u_x^d(t) &= \cos \psi(t) \sin \theta_d(t) \cos \phi_d(t) + \sin \psi(t) \sin \phi_d(t) \\ u_y^d(t) &= \sin \psi(t) \sin \theta_d(t) \cos \phi_d(t) - \cos \psi(t) \sin \phi_d(t). \end{aligned} \quad (34)$$

Due to the fact that the destination coordinates vary in time, a virtual reference vehicle with the same quadrotor helicopter mathematical model (31) is defined on the desired track, that is:

$$\dot{\hat{\mathbf{x}}}_r(t) = f(\hat{\mathbf{x}}_r(t), \hat{\mathbf{u}}_r(t)) \quad (35)$$

where $\hat{\mathbf{x}}_r(t) = [x_d(t) \ u_{0_d}(t) \ y_d(t) \ v_{0_d}(t)]'$ and $\hat{\mathbf{u}}_r(t) = [u_{x_d} \ u_{y_d}]'$ are the reference states and control inputs, respectively.

Considering the state error vector and the control input error vector defined as $\tilde{\mathbf{x}}(t) = \hat{\mathbf{x}}(t) - \hat{\mathbf{x}}_r(t)$ and $\tilde{\mathbf{u}}(t) = \hat{\mathbf{u}}(t) - \hat{\mathbf{u}}_r(t)$, the proposed translational error model is obtained from systems (31) and (35):

$$\dot{\tilde{\mathbf{x}}}(t) = \mathbf{A} \cdot \tilde{\mathbf{x}}(t) + \mathbf{B}(t) \cdot \tilde{\mathbf{u}}(t). \quad (36)$$

where matrices \mathbf{A} and $\mathbf{B}(t)$ are the Jacobians of the system (31) in relation to $\hat{\mathbf{x}}(t)$ and $\hat{\mathbf{u}}(t)$, respectively. However, to perform an appropriate path tracking in the presence of sustained disturbances, the integral of the position error should also be considered to be part of the error vector. Hence, the augmented vector error is given by:

$$\tilde{\mathbf{x}}(t) = \begin{bmatrix} \tilde{x}(t) \\ \tilde{u}_0(t) \\ \int \tilde{x}(t) dt \\ \tilde{y}(t) \\ \tilde{v}_0(t) \\ \int \tilde{y}(t) dt \end{bmatrix} = \begin{bmatrix} x(t) - x_d(t) \\ u_0(t) - u_{0_d}(t) \\ \int (x(t) - x_d(t)) dt \\ y(t) - y_d(t) \\ v_0(t) - v_{0_d}(t) \\ \int (y(t) - y_d(t)) dt \end{bmatrix} \quad (37)$$

Using Euler's method (e.g., $\dot{\tilde{x}}(t) = \frac{\tilde{x}[(k+1)\Delta t] - \tilde{x}(k\Delta t)}{\Delta t}$), the system (36) is discretized and the following model is obtained:

$$\tilde{\mathbf{x}}(k+1) = \bar{\mathbf{A}} \cdot \tilde{\mathbf{x}}(k) + \bar{\mathbf{B}}(k) \cdot \tilde{\mathbf{u}}(k). \quad (38)$$

which is time-varying and linear.

Thus, matrices $\bar{\mathbf{A}}$ and $\bar{\mathbf{B}}(k)$ are written in the discrete-time domain as follows:

$$\begin{aligned} \bar{\mathbf{A}} &= \begin{bmatrix} 1 & \Delta t & 0 & 0 & 0 & 0 \\ 0 & 1 & 0 & 0 & 0 & 0 \\ \Delta t & 0 & 1 & 0 & 0 & 0 \\ 0 & 0 & 0 & 1 & \Delta t & 0 \\ 0 & 0 & 0 & 0 & 1 & 0 \\ 0 & 0 & 0 & \Delta t & 0 & 1 \end{bmatrix} \\ \bar{\mathbf{B}}(k) &= \begin{bmatrix} 0 & 0 \\ \frac{\Delta t}{m} U_1(k) & 0 \\ 0 & 0 \\ 0 & 0 \\ 0 & \frac{\Delta t}{m} U_1(k) \\ 0 & 0 \end{bmatrix} \end{aligned} \quad (39)$$

where Δt is the sampling time, which has been chosen small enough to capture all xy motion error dynamic and high enough to consider the altitude and attitude closed-loop dynamics are in steady state.

Hence, from the xy error model the control law can be designed in such way that the system is forced to follow the reference trajectory. The idea used in this controller consists in the computation of a control law that minimizes the following cost function:

$$\begin{aligned} J &= [\hat{\tilde{\mathbf{x}}} - \tilde{\mathbf{x}}_r]^\top \mathbf{Q} [\hat{\tilde{\mathbf{x}}} - \tilde{\mathbf{x}}_r] + [\tilde{\mathbf{u}} - \tilde{\mathbf{u}}_r]^\top \mathbf{R} [\tilde{\mathbf{u}} - \tilde{\mathbf{u}}_r] \\ &\quad + \Omega (\tilde{\mathbf{x}}(k + N_2|k) - \tilde{\mathbf{x}}_r(k + N_2|k)) \end{aligned} \quad (40)$$

where \mathbf{Q} and \mathbf{R} are diagonal positive definite weighting matrices and N_2 and N_u are the prediction and control horizons, respectively [32]. Ω is the terminal state cost defined by:

$$\begin{aligned} \Omega (\tilde{\mathbf{x}}(k + N_2|k) - \tilde{\mathbf{x}}_r(k + N_2|k)) &= [\tilde{\mathbf{x}}(k + N_2|k) - \tilde{\mathbf{x}}_r(k + N_2|k)]^\top \\ &\quad \times \mathbf{P} [\tilde{\mathbf{x}}(k + N_2|k) - \tilde{\mathbf{x}}_r(k + N_2|k)] \end{aligned}$$

with $\mathbf{P} \geq 0$ [18]. The reference vectors are given by:

$$\begin{aligned} \tilde{\mathbf{x}}_r &\triangleq \begin{bmatrix} \hat{\mathbf{x}}_r(k+1|k) - \hat{\mathbf{x}}_r(k|k) \\ \vdots \\ \hat{\mathbf{x}}_r(k+N_2|k) - \hat{\mathbf{x}}_r(k|k) \end{bmatrix}, \\ \tilde{\mathbf{u}}_r &\triangleq \begin{bmatrix} \hat{\mathbf{u}}_r(k|k) - \hat{\mathbf{u}}_r(k-1|k) \\ \vdots \\ \hat{\mathbf{u}}_r(k+N_u-1|k) - \hat{\mathbf{u}}_r(k-1|k) \end{bmatrix}. \end{aligned}$$

Asymptotic stability is guaranteed for the cost function (40) if the trajectory reference is constant and no constraints are considered (see [30]). On the other hand, if the path to be followed varies on time, only asymptotic convergence can be guaranteed.

The system output predictions $\hat{\mathbf{x}}(k+j|k)$ are computed using a linear state space model of the xy movements by the Eq. (38), obtaining:

$$\hat{\mathbf{x}} = \mathbf{P}_{xy} \cdot \tilde{\mathbf{x}}(k|k) + \mathbf{H}_{xy}(k|k) \cdot \tilde{\mathbf{u}}, \quad (41)$$

where matrix \mathbf{P}_{xy} is obtained as follows:

$$\mathbf{P}_{xy} \triangleq \begin{bmatrix} \mathbf{A} \\ \mathbf{A}^2 \\ \vdots \\ \mathbf{A}^{N_2-1} \\ \mathbf{A}^{N_2} \end{bmatrix}, \quad (42)$$

and matrix \mathbf{H}_{xy} as shown at the top of the next page, where $\beta(k, j)$ is given by:

$$\beta(k, j) = \begin{cases} \mathbf{0} & \text{if } N_u = N_2 \\ \sum_{j=1}^{N_2-N_u} \mathbf{A}^{N_2-(N_u+j)} \mathbf{B}(k + (N_u + j) - 1) & \text{if } N_u < N_2 \end{cases} \quad (43)$$

$$\mathbf{H}_{xy}(k|k) \triangleq \begin{bmatrix} \mathbf{B}(k|k) & 0 & 0 & \dots & 0 \\ \mathbf{AB}(k|k) & \mathbf{B}(k+1|k) & 0 & \dots & 0 \\ \mathbf{A}^2\mathbf{B}(k|k) & \mathbf{AB}(k+1|k) & \mathbf{B}(k+2|k) & \dots & 0 \\ \vdots & \vdots & \vdots & \ddots & \vdots \\ \mathbf{A}^{N_2-1}\mathbf{B}(k|k) & \mathbf{A}^{N_2-2}\mathbf{B}(k+1|k) & \mathbf{A}^{N_2-3}\mathbf{B}(k+2|k) & \dots & \mathbf{A}^{N_2-N_u}\mathbf{B}(k+N_u-1|k) + \beta(k, j) \end{bmatrix} \quad (44)$$

By minimizing the Eq. (40) in the case where no constraints are considered, the xy motion control law can be obtained as:

$$\tilde{\mathbf{u}} = \left[\mathbf{H}'_{xy} \mathbf{Q} \mathbf{H}_{xy} + \mathbf{R} \right]^{-1} \left[\mathbf{H}'_{xy} \mathbf{Q} (\tilde{\mathbf{x}}_r - \mathbf{P}_{xy} \tilde{\mathbf{x}}(k)) + \mathbf{R} \tilde{\mathbf{u}}_r \right]. \quad (45)$$

From the computed sequence of control actions, only $\tilde{\mathbf{u}}(k|k) = [\tilde{u}_x(k|k) \ \tilde{u}_y(k|k)]'$ is needed at each instant k [4]. Thus, the control input vector is given by:

$$\begin{bmatrix} u_x^c(k) \\ u_y^c(k) \end{bmatrix} = \begin{bmatrix} \tilde{u}_x(k|k) \\ \tilde{u}_y(k|k) \end{bmatrix} + \begin{bmatrix} u_{x_d}(k) \\ u_{y_d}(k) \end{bmatrix} \quad (46)$$

Thereby, substituting the desired virtual input value, \mathbf{u}_{xy}^d , from the computed one obtained with Eq. (46), the roll and pitch reference angles, ϕ_d and θ_d respectively, are derived using Eq. (34). These references are necessary for the helicopter inner-loop controller.

6. Simulation Results

Simulations have been performed in order to test the proposed control strategy when the quadrotor helicopter executes some path following. The performance obtained by this strategy have been checked considering a more accurate model, which emulates a real quadrotor helicopter. This model takes into account the crossed inertia terms in the moment of inertia tensor as well as saturated control inputs. This fact implies that structural uncertainty has been considered with respect to the simplified nominal model used for control synthesis purposes. Besides, an amount of $\pm 40\%$ in the uncertainty of the elements of the moment of inertia tensor and the mass has also been considered to test the robustness provided by the control strategy with respect to parametric uncertainty. Finally, sustained disturbances affecting all the degrees of freedom have been applied in different instants of time to check the disturbance rejection capability of the proposed control strategy.

The following vertical helix has been defined as the first reference trajectory (see Fig. 3):

$$x_d = \frac{1}{2} \cos\left(\frac{t}{2}\right) m, \quad y_d = \frac{1}{2} \sin\left(\frac{t}{2}\right) m, \\ z_d = 1 + \frac{t}{10} m, \quad \psi_d = \frac{\pi}{3} rad$$

The helicopter initial conditions are $\xi_0 = [0 \ 0 \ 0.5]'$ m and $\eta_0 = [0 \ 0 \ 0.5]'$ rad. The values of the model nominal parameters used for simulations are shown in Table 1.

The following persistent steps have been applied as aerodynamic moments and forces disturbances in the simulations: $A_r = 1$ Nm at $t = 5$ s; $A_z = -1$ N at $t = 10$ s; $A_p = 1$ Nm at $t = 15$ s; $A_x = 1$ N at $t = 20$ s; $A_q = 1$ Nm at $t = 25$ s and $A_y = 1$ N at $t = 30$ s.

Table 1. QuadRotor helicopter model parameters.

Parameter Description	Parameter	Value
Mass of the quadRotor helicopter	m	0.74 kg
Distance between the mass center and the rotors	l	0.21 m
Gravitational acceleration	g	9.81 m/s ²
Moment of inertia around the x -axis	I_{xx}	0.004 kg.m ²
Moment of inertia around the y -axis	I_{yy}	0.004 kg.m ²
Moment of inertia around the z -axis	I_{zz}	0.0084 kg.m ²

The MPC parameters were adjusted as follows:

$$N_2 = 6, \quad N_u = 3,$$

$$Q = \begin{bmatrix} 5 & 0 & 0 & 0 & 0 & 0 \\ 0 & 5 & 0 & 0 & 0 & 0 \\ 0 & 0 & 10 & 0 & 0 & 0 \\ 0 & 0 & 0 & 5 & 0 & 0 \\ 0 & 0 & 0 & 0 & 5 & 0 \\ 0 & 0 & 0 & 0 & 0 & 10 \end{bmatrix}, \quad R = \begin{bmatrix} 65 & 0 \\ 0 & 65 \end{bmatrix}$$

The nonlinear \mathcal{H}_∞ controller gains were tuned with the following values: $\omega_1 = 0.1$, $\omega_2 = 3$, $\omega_3 = 9$ y $\omega_u = 1.5$. In addition, a simulation using $\omega_3 = 0$ was performed in order to show the integral action improvement on the inner-loop control.

Figs 3 to 7 indicate an excellent reference tracking performance even if external disturbances originated by aerodynamic forces and moments are considered. These results illustrate the robust behavior provided by the outer-inner control structure in the case of both parametric and structural uncertainty.

The smooth reference tracking provided by the MPC can be observed in Figs 4 and 5. This fact is clearly visible at the beginning of the trajectory where the vehicle is far from the reference. This is due to the fact that the predictive controller considers the future reference in the computation of the control signal so as to predict a path that would result in a softer displacement.

The time evolution of the translational position and its error are shown in Figs 4 and 5 respectively. The integral action features of the MPC controller can be easily observed in Fig. 5. This integral action makes it possible to obtain null error in the path tracking when sustained disturbances affect the xy motion of the helicopter.

An additional simulation considering the integral action weighting of the inner-loop, ω_3 , equal to zero is also plotted in the graphs. This simulation shows the deterioration

in the tracking performance when this action is not taken into account, since the inner-loop controller is not able to reject the sustained disturbances acting on the helicopter. In Fig. 5 it can be observed that the outer-loop controller manages to obtain xy error null in the presence of external disturbances in the case of the integral action weighting of the inner-loop is null. However, the altitude, that is a variable controlled by the nonlinear \mathcal{H}_∞ controller, maintains a constant offset during all the trajectory.

Figs 6 and 7 illustrate the Euler angles evolution. In these graphs a Euler angles steady-state error can also be observed in the trajectory that the integral action weighting, ω_3 , is equal to zero. In this case, apart from the fact that the inner-loop loses performance, it is interesting to note that the outer-loop controller tries to compensate for the lack of integral action by increasing the ϕ and θ reference angles.

Another simulation collection has been provided in order to corroborate the improvements reached by the proposed control structure in this study when compared with the one of same authors published in [29]. This strategy makes use of the uncoupled quadrotor model, when two controllers designed for fully actuated systems are implemented. The reference trajectory used is a circle evolving in \mathbb{R}^3 Cartesian space defined by:

$$x_d = \frac{1}{2} \cos\left(\frac{\pi t}{20}\right) m, \quad y_d = \frac{1}{2} \sin\left(\frac{\pi t}{20}\right) m,$$

$$z_d = 3 - 2 \cos\left(\frac{\pi t}{20}\right) m, \quad \psi_d = \pi/3 \text{ rad}$$

The UAV started from $\xi_0 = [0 \ 0.2 \ 0.5]'m$ and $\eta_0 = [0 \ 0 \ 0.5]'rad$ with a parametric uncertainty of 40% in the elements of the moment of inertia tensor and the mass. The controller parameters defined before have also been used in these simulations in both control structures, being necessary to synthesize just the altitude controller parameters used in [29], which have been adjusted to present a similar performance with respect to the compared control strategy. The simulation results are illustrated in Figs 8 to 12.

These figures show that both control strategies present a robust path following when parametric uncertainties and sustained disturbances are applied to the system. In order to make a quantitative comparison of the results obtained by these two control strategies, the Integral Square Error (ISE) performance indexes, presented in Table 2, have been computed from the simulation results showed in Figs 8 to 12. Results obtained considering the quadrotor helicopter model (6–7) with nominal parameters have presented very similar ISE performance indexes. However, when an amount of 40% in the uncertainty of parameters of the moment of inertia tensor and the mass has been considered, a large improvement has

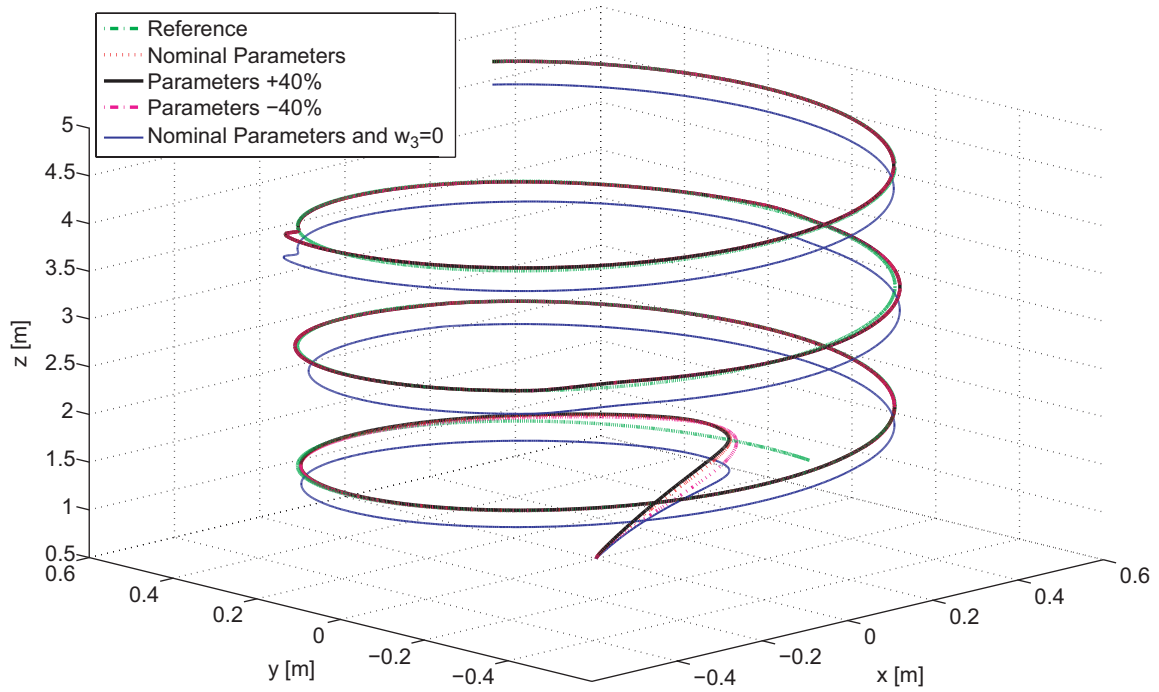


Fig. 3. Path following with external disturbances.

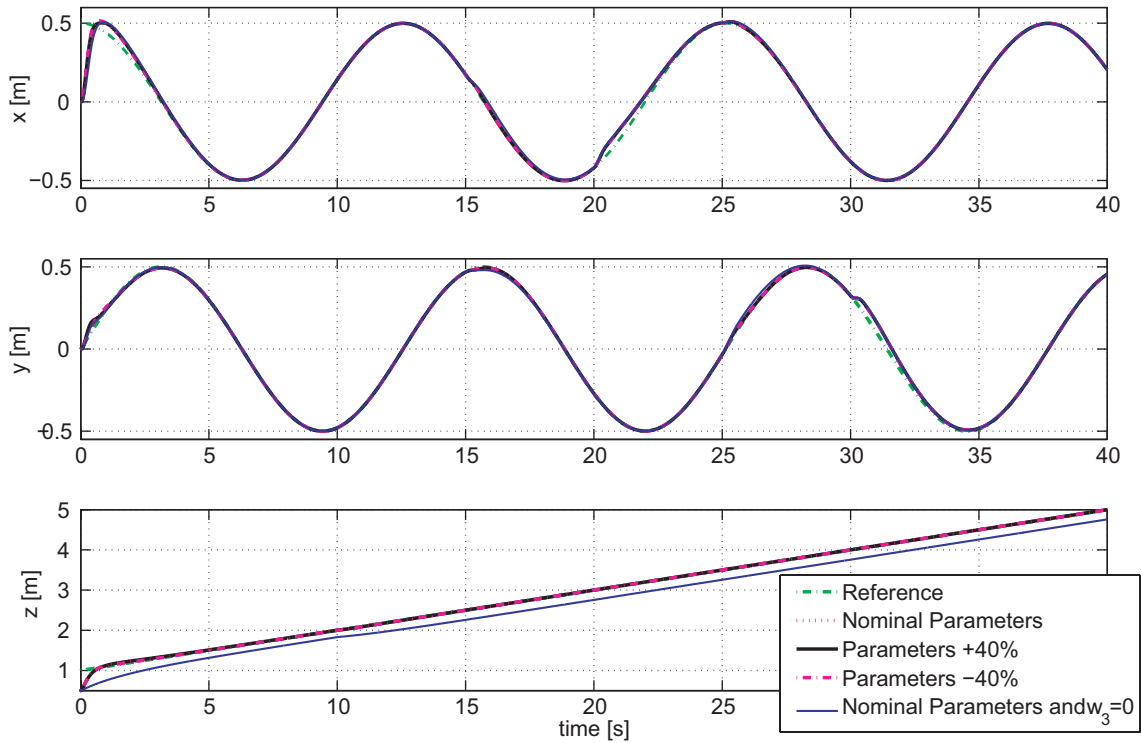


Fig. 4. Position (x, y, z) with external disturbances.

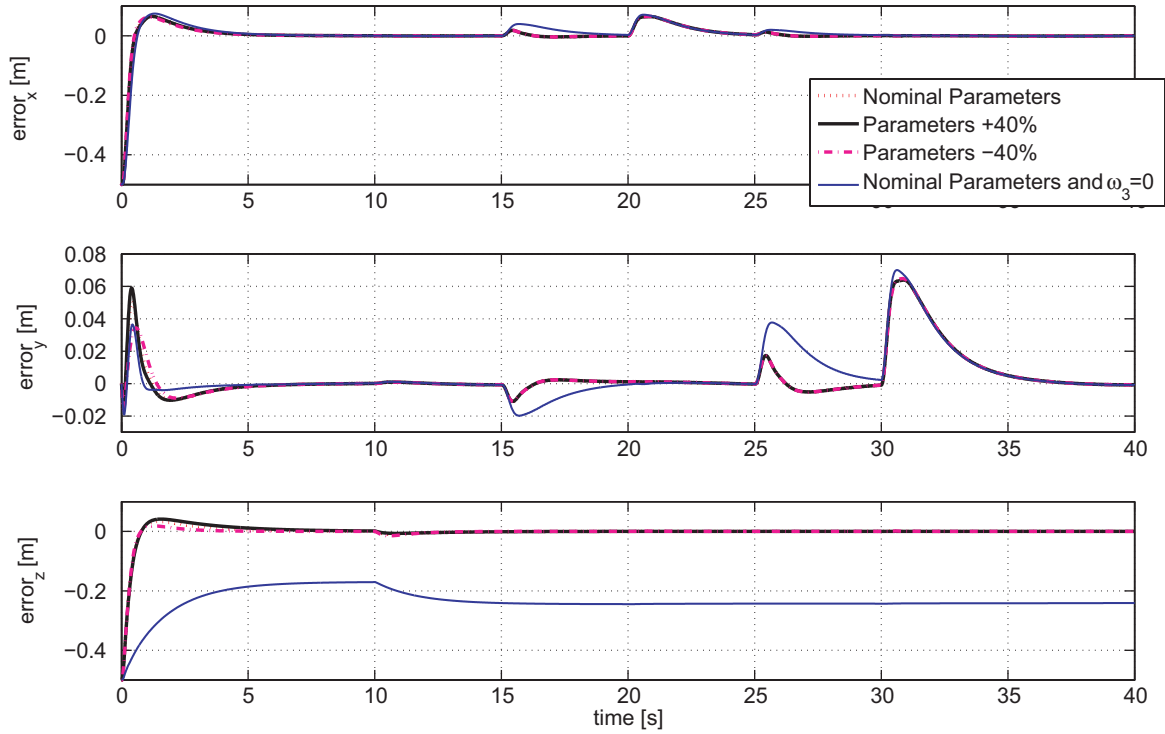


Fig. 5. Position error (x, y, z) with external disturbances.

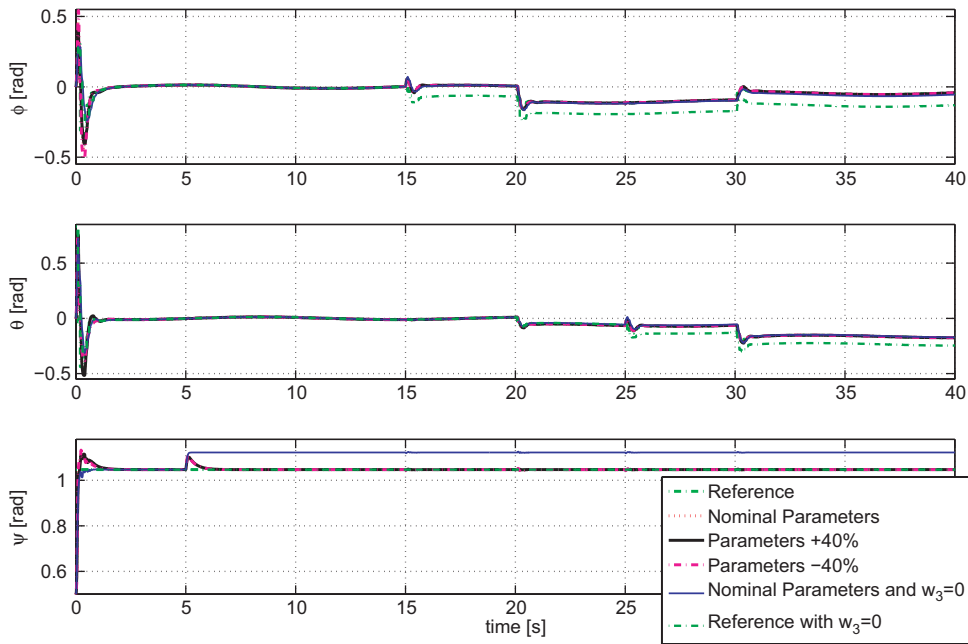


Fig. 6. Orientation (ϕ, θ, ψ) with external disturbances.

been achieved by the proposed control structure. It can be observed that the performance is improved by the MPCxy + UnderActuatedNonlinear \mathcal{H}_∞ control strategy for most of states ($x \downarrow 17.64\%$, $y \downarrow 26.39\%$, $z \downarrow 40.81\%$,

$\phi \downarrow 103.09\%$, $\theta \downarrow 183.12\%$ and $\psi \uparrow 1.71\%$). These better results, when uncertainties parametric are considered, are due to the underactuated nonlinear \mathcal{H}_∞ structure used. It computes the applied control inputs taking into account

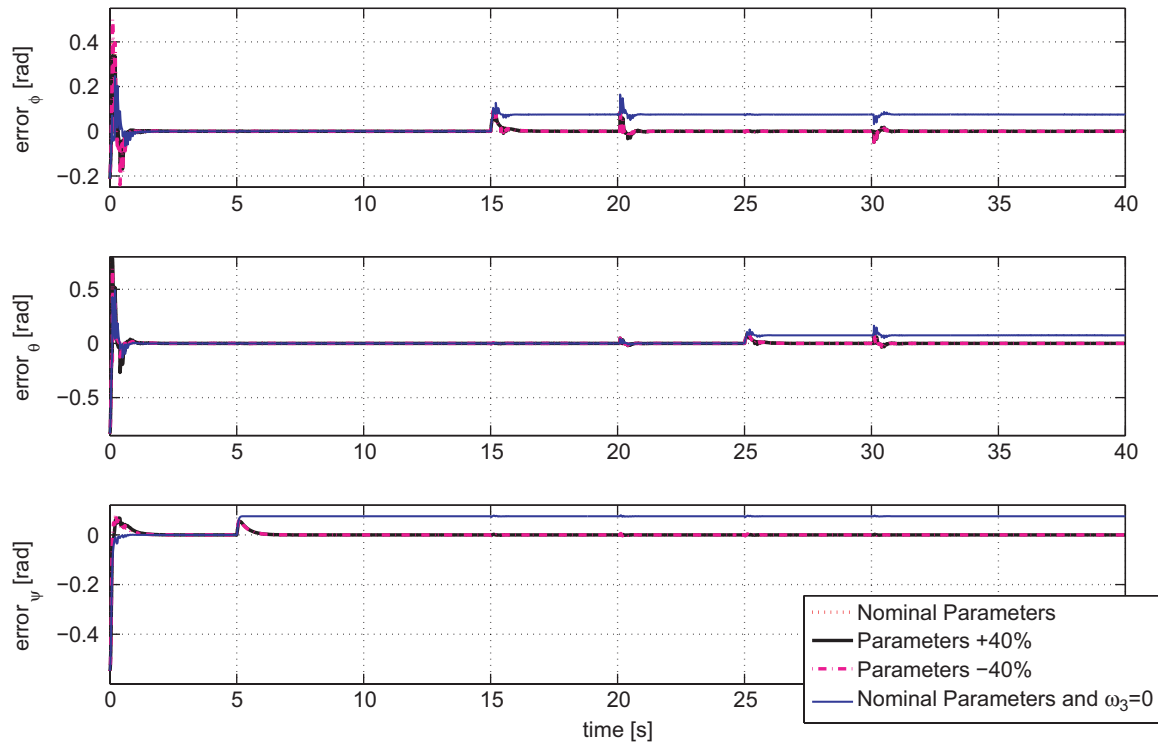


Fig. 7. Orientation error (ϕ, θ, ψ) with external disturbances.

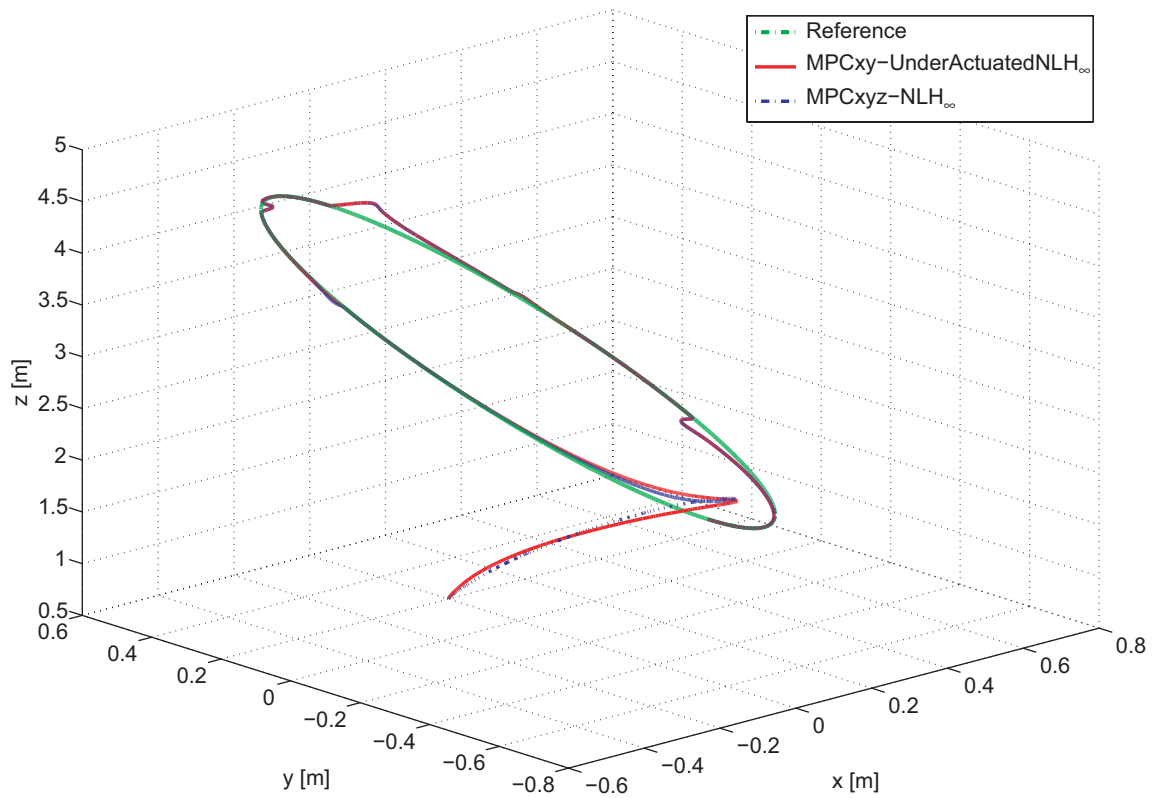


Fig. 8. Path following.

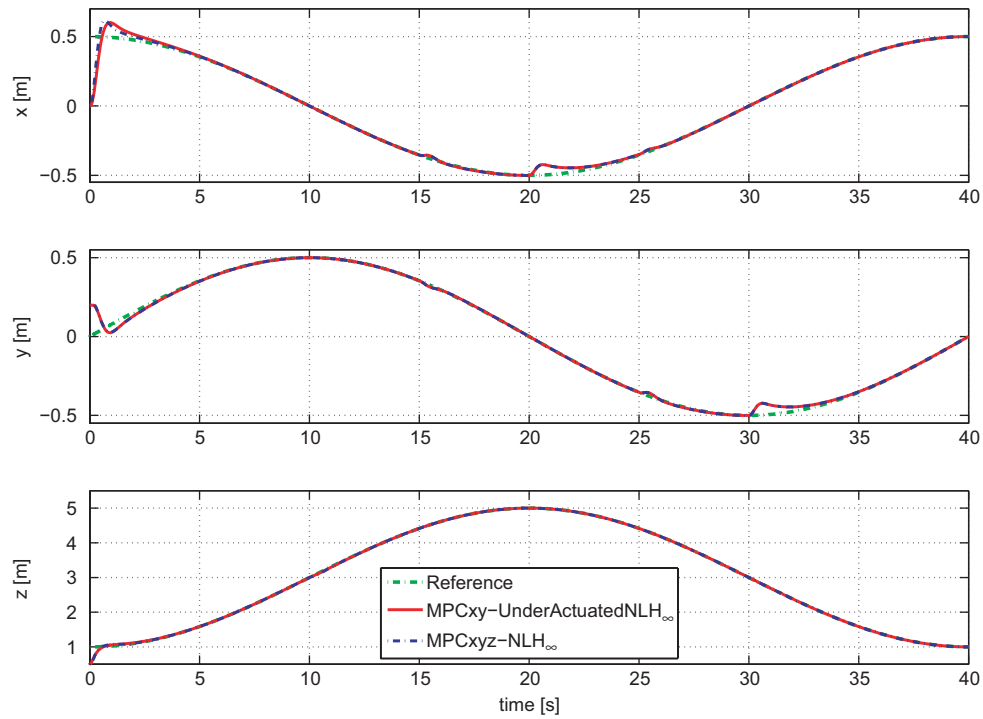


Fig. 9. Position (x, y, z) .

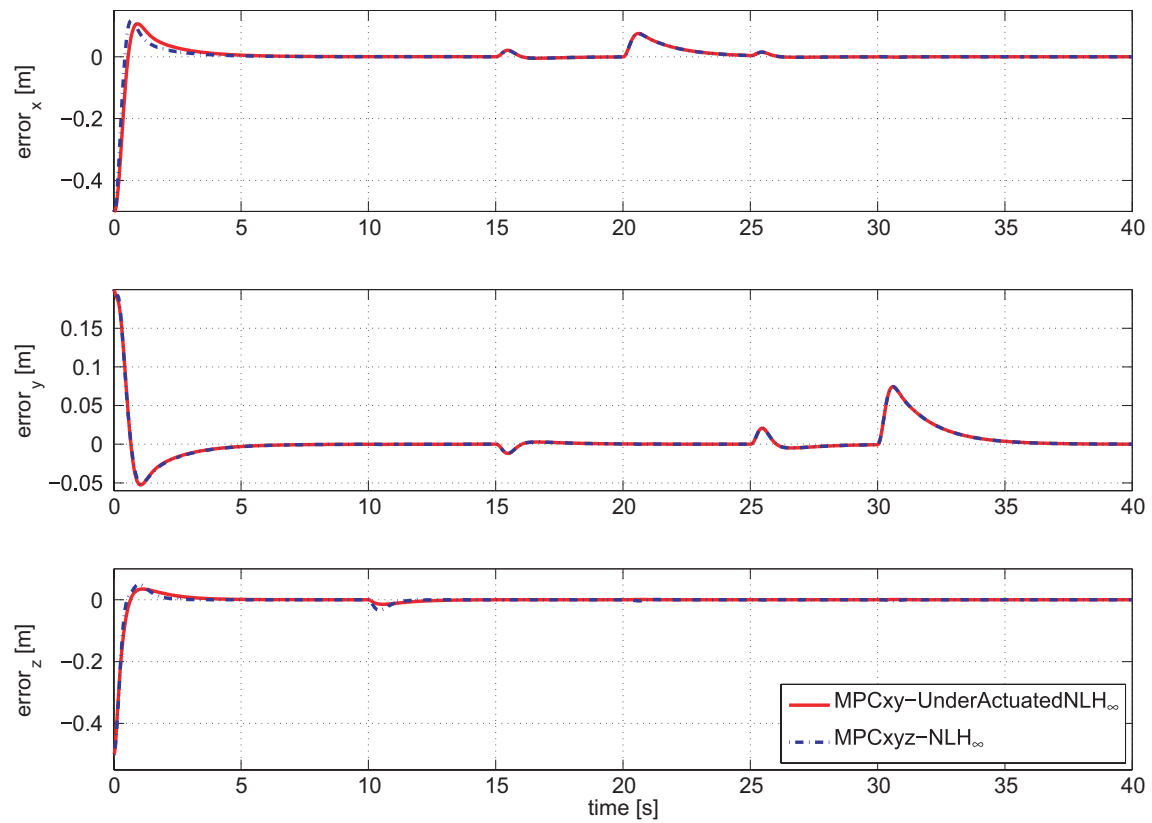


Fig. 10. Position error (x, y, z) .

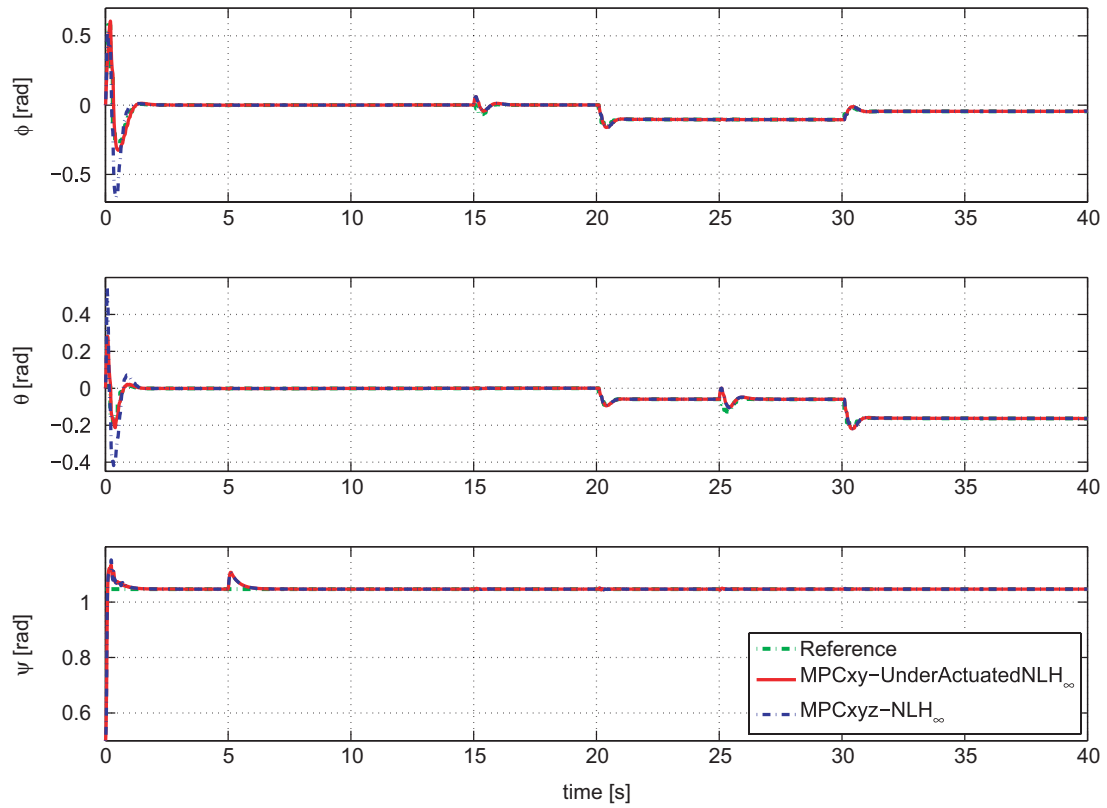


Fig. 11. Orientation (ϕ, θ, ψ).

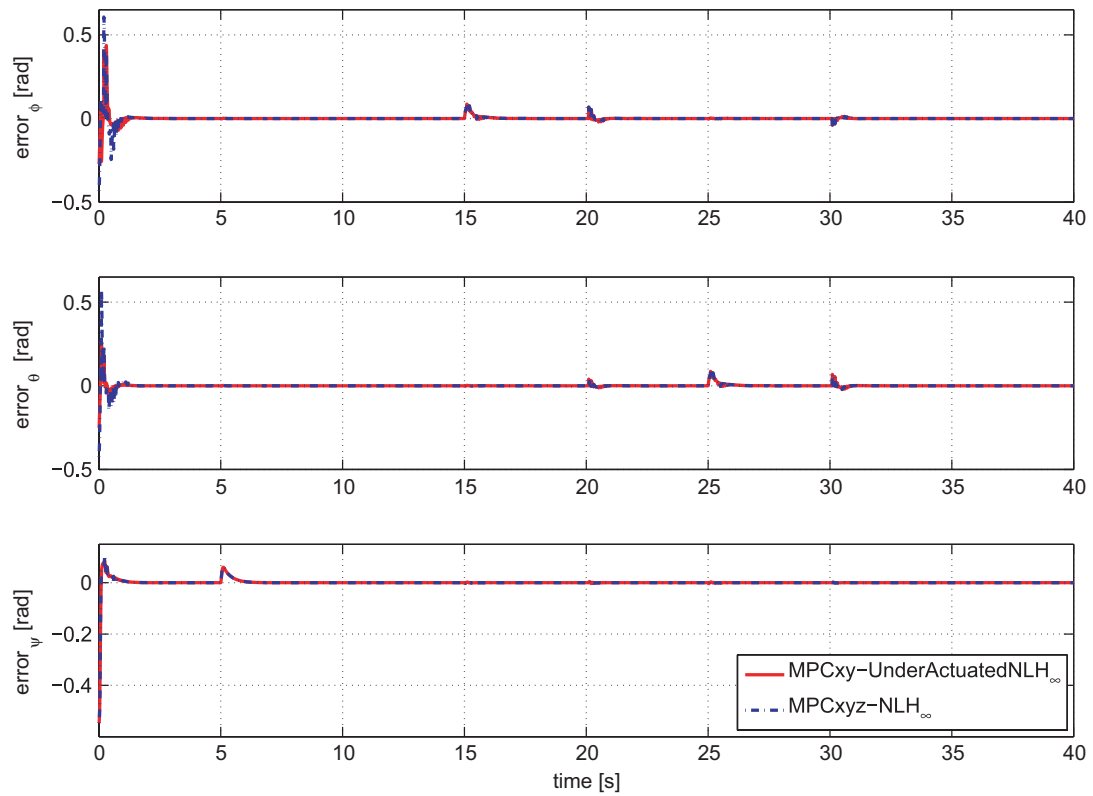


Fig. 12. Orientation error (ϕ, θ, ψ).

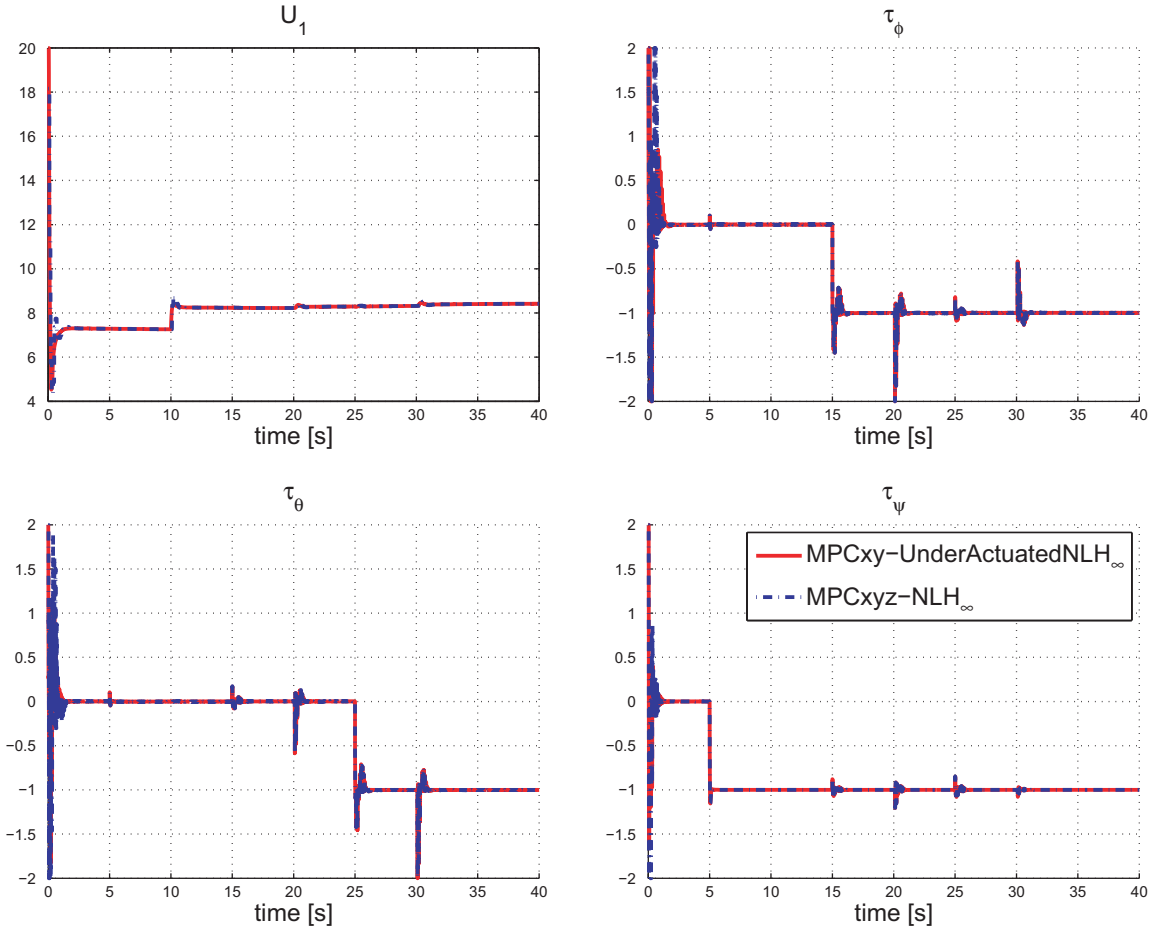


Fig. 13. Control inputs ($U_1, \tau_{\phi_a}, \tau_{\theta_a}, \tau_{\psi_a}$).

Table 2. ISE Index Performance Analysis.

States	MPCxy + UnderActuatedNL \mathcal{H}_∞	MPCxyz + NL \mathcal{H}_∞
x	14.3968	16.9365
y	3.2658	4.1275
z	10.1827	14.3379
ϕ	4.3876	8.9109
θ	1.8097	5.1237
ψ	5.9508	5.8488

the noncontrolled DOF, that is, the uncertainty on the mass that affect the xy motion is also counterattacked by the inner-controller loop. Meanwhile, with the controller proposed in [29], this effect is only just considered as an unknown external disturbance.

7. Conclusions

In this study an underactuated nonlinear \mathcal{H}_∞ control to compute the applied control actions on the quadrotor

helicopter has been presented. This controller is based on the 6DOF quadrotor helicopter model that provides a control law with knowledge of both the active degrees of freedom and the passive ones.

To solve the path tracking problem, an outer-loop controller has been implemented which is used as a track generator. That is, using a previously known path reference, an MPC based on the xy motion error model is designed to generate the necessary ϕ and θ reference angles. To perform the sustained disturbance rejection, the integral term of the xy position error has been included in the error vector. Moreover, because of the predictive controller features, a good and smooth performance in the xy plane reference tracking is achieved.

The robust performance provided by the inner-outer control strategy has been tested by simulation. A more accurate helicopter model than the one used for control synthesis purposes has been employed to obtain simulation results, which introduces structural uncertainty in the problem. Besides, an amount of 40% of uncertainty has been considered in several mechanical parameters of the vehicle, and some sustained disturbances on all the degrees

of freedom have been applied during the simulations. Despite these facts, an excellent tracking performance has been achieved with the proposed control structure.

Acknowledgments

The authors thank CICYT for funding this work under grants DPI2006-07338 and DPI2007-64697.

References

1. Altug E, Ostrowski JP, Mahony R. Control of a quadrotor helicopter using visual feedback. In *Proc 2002 IEEE Int Conf Robotics Automation*, pages 72–77, Washington, DC, 2002
2. Bouabdallah S, Siegwart R. Backstepping and sliding-mode techniques applied to an indoor micro quadrotor. In *Proc IEEE Int Conf on Robot Automat*, pages 2259–2264, Barcelona, Spain, 2005
3. Bouabdallah S, Siegwart R. Full control of a quadrotor. In *Proc Intelligent Robots Syst. IROS 2007*, pages 153–158, San Diego, USA, 2007
4. Camacho EF, Bordons C. *Model Predictive Control*. Springer-Verlag, New York, 1998
5. Castillo P, García P, Lozano R, Albertos P. Modelado y Estabilización de un Helicóptero con Cuatro Rotores. *RIAI Revista Iberoamericana de Automática e Informática Industrial*, 2007; 4(1): 41–57
6. Castillo P, Lozano R, Dzul A. Stabilization of a mini rotorcraft with four rotors. *IEEE Cont Syst Mag*, 2005: 45–55
7. Castillo P, Lozano R, Dzul AE. *Modelling and Control of Mini-Flying Machines*. Springer-Verlag, London, 2005
8. Chen BS, Lee TS, Feng JH. A nonlinear \mathcal{H}_∞ control design in robotic systems under parameter perturbation and external disturbance. *Int J Control*, 1994; 59(2): 439–461
9. Chen M, Huzmezan M. A combined MBPC/2DOF \mathcal{H}_∞ controller for a quad rotor UAV. In *Proc AIAA Guidance, Navigation, and Control Conference and Exhibit*, Texas, USA, 2003
10. Fantoni I, Lozano R. *Non-linear Control for Underactuated Mechanical Systems*. Springer-Verlag, London, 2002
11. Feng W, Postlethwaite I. Robust nonlinear H_∞ /adaptive control of robot manipulator motion. *Proc Instn Mech Engrs*, 1994; 208: 221–230
12. Frazzoli E, Dahleh MA, Feron E. Trajectory tracking control design for autonomous helicopters using a backstepping algorithm. In *Proc Am Control Conference*, 6, pages 4102–4107, 2000
13. Guenard N, Hamel T, Mahony R. A practical visual servo control for an unmanned aerial vehicle. *Robotics, IEEE Trans [see also Robotics and Automation, IEEE Transactions on]*, 2008; 24(2): 331–340
14. Guisser M, Medromi H, Ifassiouen H, Saadi J, Radhy N. A coupled nonlinear discrete-time controller and observer designs for underactuated autonomous vehicles with application to a quadrotor aerial robot. In *Proc 33rd IEEE-IECON06*, pages 1–6, Paris, France, 2006
15. Hoffmann GM, Huang H, Waslander SL, Tomlin CJ. Quadrotor helicopter flight dynamics and control: Theory and experiment. In *Proc AIAA Guidance, Navigation and Control Conf Exhibit*, pages 1–20, South Carolina, USA, 2007
16. Isidori A, Marconi L, Serrani A. *Robust Autonomous Guidance*. Springer-Verlag, New York, Secaucus, NJ, 2003
17. Johansson R. Quadratic optimization of motion coordination and control. *IEEE Trans Automatic Cont*, 1990; 35(11): 1197–1208
18. Kuhne F, Lages WF, Da Silva JMG. Point stabilization of mobile robots with nonlinear model predictive control. In *Proc IEEE Mechatronics Robotics*, volume 3, pages 1163–1168, Niagara Falls, Canada, 2005
19. López-Martínez M, Ortega MG, Rubio FR. Nonlinear L_2 control of a laboratory helicopter with variable speed rotors. *Automatica*, 2007; 43(4): 655–661
20. Metni N, Hamel T, Derkx F. Visual tracking control of aerial robotic systems with adaptive depth estimation. In *Proc CDC/ECC*, pages 6078–6084, Seville, Spain, 2005
21. Mistler V, Benallegue A, M'Sirdi NK. Exact linearization and noninteracting control of a 4 rotors helicopter via dynamic feedback. In *Proc IEEE Int Workshop Robot Human Inter Commun*, 2001
22. Mokhtari A, Benallegue A, Daachi B. Robust feedback linearization and \mathcal{H}_∞ Controller for a quadrotor unmanned aerial vehicle. *J Elect Eng*, 2006; 57(1): 20–27
23. Mokhtari A, Benallegue A, Orlov Y. Exact linearization and sliding mode observer for a quadrotor unmanned aerial vehicle. *Int J Robotics Autom*, 2006; 21(1): 39–49
24. Olfati-Saber R. *Nonlinear Control of Underactuated Mechanical Systems with Application to Robotics and Aerospace Vehicles*. PhD thesis, Massachusetts Institute of Technology, 2001
25. Ortega MG, Vargas M, Vivas C, Rubio FR. Robustness improvement of a nonlinear H_∞ controller for robot manipulators via saturation functions. *J Robotic Syst*, 2005; 22(8): 421–437
26. Raffo GV, Ortega MG, Rubio FR. Nonlinear \mathcal{H}_∞ Control applied to the personal pendulum car. In *Proc Eur Control Conf. ECC'07*, Kos, Greece, 2007
27. Raffo GV, Ortega MG, Rubio FR. Backstepping/nonlinear \mathcal{H}_∞ Control for path tracking of a quad-rotor unmanned aerial vehicle. In *Proc 2008 Am Control Conf—ACC2008*, pages 3356–3361, Seattle, USA, June 2008
28. Raffo GV, Ortega MG, Rubio FR. MPC with nonlinear \mathcal{H}_∞ Control for path tracking of a quad-rotor helicopter. In *Proc 17th IFAC World Congress 2008—IFAC'08*, pages 8564–8569, Seoul, Korea, 2008
29. Raffo GV, Ortega MG, Rubio FR. An integral predictive/nonlinear \mathcal{H}_∞ control structure for a quadrotor helicopter. *Automatica*, 2010; 46: 29–39
30. Rawlings JB, Mayne DQ. *Model Predictive Control: Theory and Design*. Nob Hill Publishing, Madison, 2009
31. Roberts JF, Stirling T, Zufferey JC, Floreano D. Sensing for autonomous indoor flight. In *Proc Eur Micro Air Vehicle Conf Flight Competition (EMAV)*, 2007
32. Rossiter JA. *Model-Based Predictive Control: A Practical Approach*. CRC Press, New York, 2003
33. Siqueira AAG, Terra MH. Nonlinear \mathcal{H}_∞ control for underactuated manipulators with robustness tests. *Revista de Control & Automação*, 2004; 15(3): 339–350
34. Siqueira AAG, Terra MH, Maciel BCO. Nonlinear mixed $\mathcal{H}_2/\mathcal{H}_\infty$ control applied to manipulators via actuation redundancy. *Control Eng Pract*, 2006; 14: 327–335

35. Tournier GP, Valenti M, How JP, Feron E. Estimation and control of a quadrotor vehicle using monocular vision and Moir'e patterns. In *Proc AIAA Guidance, Navigation, and Control Conf Exhibit*, August 2006
36. Van der Schaft A. L_2 -gain analysis of nonlinear systems and nonlinear state feedback control. *IEEE Trans Automat Control*, 1992; 37(6): 770–784
37. Van der Schaft A. *L_2 -Gain and Passivity Techniques in Nonlinear Control*. Springer-Verlag, New York, 2000
38. Xu R, Ozg uner U. Sliding mode control of a quadrotor helicopter. In *Proc 45th IEEE Conf Decision Control*, pages 4957–4962, San Diego, USA, 2006
39. Xu R, Özgüner Ü. Sliding mode control of a class of underactuated systems. *Automatica*, 2008, 44: 233–241
40. Zemalache KM, Beji L, Maaref H. Two inertial models of x4-flyers dynamics, motion planning and control. *Integrated Computer-Aided Eng*, 2007; 14(2): 107–119